© 2017. Published by The Company of Biologists Ltd | Journal of Cell Science (2017) 130, 344-359 doi:10.1242/jcs.193086

RESEARCH ARTICLE

Drosophila WASH is required for integrin-mediated cell adhesion, cell motility and lysosomal neutralization

Benedikt M. Nagel[1,2], Meike Bechtold[1], Luis Garcia Rodriguez[1] and Sven Bogdan[1,2,*]

ABSTRACT

The Wiskott-Aldrich syndrome protein and SCAR homolog (WASH; also known as Washout in flies) is a conserved actin-nucleation-promoting factor controlling Arp2/3 complex activity in endosomal sorting and recycling. Previous studies have identified WASH as an essential regulator in *Drosophila* development. Here, we show that homozygous *wash* mutant flies are viable and fertile. We demonstrate that *Drosophila* WASH has conserved functions in integrin receptor recycling and lysosome neutralization. WASH generates actin patches on endosomes and lysosomes, thereby mediating both aforementioned functions. Consistently, loss of WASH function results in cell spreading and cell migration defects of macrophages, and an increased lysosomal acidification that affects efficient phagocytic and autophagic clearance. WASH physically interacts with the vacuolar (V)-ATPase subunit Vha55 that is crucial to establish and maintain lysosome acidification. As a consequence, starved flies that lack WASH function show a dramatic increase in acidic autolysosomes, causing a reduced lifespan. Thus, our data highlight a conserved role for WASH in the endocytic sorting and recycling of membrane proteins, such as integrins and the V-ATPase, that increase the likelihood of survival under nutrient deprivation.

KEY WORDS: *Drosophila*, WASH, Actin cytoskeleton, Cell adhesion, Lysosome neutralization, Macrophages, Arp2/3, Wiskott-Aldrich syndrome, V-ATPase, Integrin

INTRODUCTION

The Wiskott-Aldrich syndrome protein (WASP) family of nucleation promoting factors (NPF) controls actin dynamics by activating the ubiquitous Arp2/3 complex, a nucleation machinery that initiates actin filament branches on the sides of pre-existing filaments. One of three highly conserved WASP-family members is the Wiskott-Aldrich syndrome protein and SCAR homolog (WASH; CG13176 in flies) protein that is found across multiple eukaryotic kingdoms (Veltman and Insall, 2010). As all class-I NPFs, WASH possesses a VCA domain at its C-terminal end that activates the Arp2/3 complex *in vitro* (Linardopoulou et al., 2007). It differs considerably from other members of this class at its N-terminal part as it has a WASH-homology domain (WAHD), comprising a WASH homology domain 1 (WAHD1) and a tubulin-binding region (TBR) (Gomez and Billadeau, 2009). In cells, WASH exists in a stable pentameric complex known as the WASH regulatory complex (SHRC) that contains four additional subunits: strumpellin (encoded by *KIAA0196*), FAM21, SWIP (encoded by *WSB1*) and CCDC53. This complex appears to be structurally very similar to the WAVE regulatory complex (WRC), which controls the activity and localization of WAVE (Jia et al., 2010). Similar to the WRC, knockdown of individual WASH complex subunits results in the degradation of other WASH complex components (Derivery et al., 2009; Gomez and Billadeau, 2009; Jia et al., 2010). However, the SHRC seems to be constitutively active in contrast to the WRC, thus possibly being regulated by, so far, unknown mechanisms (Derivery and Gautreau, 2010; Gomez and Billadeau, 2009).

First insights into the cellular function of WASH-mediated actin polymerization emerged from the subcellular localization of WASH and from RNA interference (RNAi) studies in mammalian cell culture. These studies have demonstrated that WASH is an endosomal protein that regulates several sorting and maturation steps of endocytic vesicles. Upon WASH depletion, endosomes change shape from normally spherical to an enlarged and tubular shape (Derivery et al., 2009; Duleh and Welch, 2010; Gomez and Billadeau, 2009), indicating that WASH plays a role in regulating endosome tubulation and scission. WASH colocalizes with Rab4, Rab7 and Rab11, suggesting an important role in both early and late endosomal recycling pathways (Derivery et al., 2009). In line with this notion, *wash*-deficient cells show trafficking defects in different endocytic routes, including endosome-to-Golgi transport through the retromer complex (Gomez and Billadeau, 2009; Harbour et al., 2012; Duleh and Welch, 2012; Piotrowski et al., 2013; Zech et al., 2011) and endosome-to-plasma-membrane recycling of various cargos, such as integrins and the epidermal growth factor (EGF) and transferrin receptors (Derivery et al., 2009; Zech et al., 2011). Thus, WASH activity is thought to facilitate and maintain the segregation of endosomal sorting domains.

First evidence for the *in vivo* role of WASH in lysosomal maturation and autophagy comes from loss-of-function studies in *Dictyostelium* (Carnell et al., 2011). Normally, endosomes and, in particular, lysosomes get acidified by the activity of the vacuolar (V)-ATPase, a large multimeric ATP-dependent H^+ pump (Maxson and Grinstein, 2014). An acidic environment provides not only an optimal pH for a wide range of acidic hydrolases but also ensures that internalized receptors release their ligands so that they can recycle back to the plasma membrane (Luzio et al., 2007; Pryor and Luzio, 2009). Dissociated ligands are then delivered to late endosomes, whereas the receptors are sorted into recycling vesicles destined for the plasma membrane. The successive acidification of endosomes further leads to highly acidic lysosomes where proteins are degraded.

Before exocytosis of indigestible material can occur, lysosomes have to be neutralized by retrieving the V-ATPase from the lysosomal membrane. This task is performed by WASH, as it interacts with the V-ATPase and generates a newly polymerized network that, in turn, pushes the V-ATPase out of the membrane

[1]Institut für Neurobiologie, Universität Münster, Badestr. 9, 48149 Münster, Germany. [2]Institut für Physiologie und Pathophysiologie, Abteilung Molekulare Zellphysiologie, Phillips-Universität Marburg, Emil-Mannkopff-Straße 2, 35037 Marburg, Germany.

*Author for correspondence (sbogdan@uni-muenster.de)

S.B., 0000-0002-8753-9855

Received 26 May 2016; Accepted 8 November 2016

Journal of Cell Science (2017) 130, 344-359 doi:10.1242/jcs.193086

(Carnell et al., 2011). Lysosomal neutralization requires a functional WASH-VCA domain, suggesting that Arp2/3-mediated actin polymerization is essential for the V-ATPase retrieval (Carnell et al., 2011). Further studies in *Dictyostelium* and in mammalian cells suggest a conserved role of WASH in regulating the lysosomal network required for efficient phagocytic and autophagic digestion (Kolonko et al., 2014; King et al., 2013; Gomez et al., 2012). *Dictyostelium* cells lacking WASH are unable to digest their cytoplasm in order to survive phases of starvation (King et al., 2013). The phenotypic analysis of *wash* knockout mice confirms an important *in vivo* function of WASH in regulating autophagy (Xia et al., 2014). WASH deficiency results in embryonic lethality and mutant mice show extensive autophagy (Xia et al., 2014). Therefore, a model has been proposed in which WASH inhibits autophagy by suppressing ubiquitination of Beclin1/Atg 6, a core component of the conserved Vps34 complex, which promotes autophagosome formation when active (Xia et al., 2014). Remarkably, different from its activity in V-ATPase retrieval and retromer-mediated endosomal sorting, the function of WASH in autophagy does not require its Arp2/3-activating activity. A truncated WASH protein lacking the VCA domain still rescues the accelerated autophagy induction in *wash*−/− mouse embryonic fibroblasts similar to full-length WASH (Xia et al., 2014). Surprisingly, rather than finding accelerated autophagy, Zavodszky and colleagues have recently reported impaired autophagy in HeLa cells that had been depleted for WASH (Zavodszky et al., 2014a,b). Thus, the exact role of WASH as an NPF in autophagy remains unclear so far.

In *Drosophila*, a role of WASH (known as Washout in flies) in lysosomal function and autophagy has not been reported yet. The initial analysis of a deletion mutant suggests an essential function of WASH in *Drosophila* oogenesis and larval development (Linardopoulou et al., 2007; Liu et al., 2009). However, whether the observed lethality and the oogenesis defects are due to a loss of WASH function has not been addressed in these studies. The role of WASH in developmental dispersal of immune cells during *Drosophila* embryogenesis is even unclear. RNAi-mediated knockdown of WASH partially affects the stereotypic migration of embryonic macrophages (Verboon et al., 2015), but the loss-of-function mutant macrophages are indistinguishable from wild type (Evans et al., 2013). By contrast, a more recent study demonstrates a conserved function in retromer-dependent endocytic recycling of the luminal protein Serpentine in *Drosophila* trachea development (Dong et al., 2013). *wash* mutant embryos show defects in tracheal tube length, phenocopying *rab9* and *vps35* mutants (Dong et al., 2013).

Here, we analyzed the function of WASH in *Drosophila*. Different from previous studies, we show that WASH is dispensable for *Drosophila* development. Viable mutant females show neither reduced fertility nor defects in the morphology of developing egg chambers. Instead, we found a requirement of WASH in integrin-dependent cell spreading of macrophages, and we provide further evidence for a conserved role in generating F-actin patches, in driving late endosomal recycling and in lysosome neutralization that is required for efficient phagocytic and autophagic clearance.

RESULTS

Homozygous *wash* mutants are viable and have no defects in oogenesis

The *Drosophila melanogaster* genome contains a single *wash* gene located on the second chromosome (2R) at the cytological location 48E6 (Fig. 1A). It consists of a single exon encoding a 75-kDa protein. In previous studies, a *wash* deletion mutant (*wash*Δ185) was generated through imprecise excision of the P-element EY15549 inserted between codon 11 and 12 of the *wash* open reading frame (ORF) (Linardopoulou et al., 2007). We confirmed the 1029-bp deletion in *wash*Δ185 mutant flies (Fig. 1B; Linardopoulou et al., 2007). This deletion removes more than half of the coding region, resulting in a premature stop codon. Flies homozygous for this deletion chromosome die at the late third-instar larvae stage, indicating an essential function of WASH in *Drosophila* development (Linardopoulou et al., 2007; Liu et al., 2009). However, whether the lethality is due to a loss of WASH function was not addressed in those studies (Linardopoulou et al., 2007; Liu et al., 2009). The existence of viable flies bearing the 10-kb P-element insertion EY15549 in the *wash* ORF already suggests that the lethality of homozygous *wash*Δ185 mutant animals might be caused by second-hit mutations. This discrepancy prompted us to test trans-heterozygous flies with the sequence-mapped deficiency Df(2R)BSC699, which removes the complete *wash* gene locus (Fig. 1A,B).

Trans-heterozygous *wash*Δ185/Df(2R)BSC699 flies, but also the homozygous viable P-element insertion strain, completely lacked WASH expression (Fig. 1C). Remarkably, they were viable with no apparent developmental defects, suggesting that lethality was caused by a second-site mutation. Consistently, we could establish a viable *wash* mutant fly stock (termed *wash*Δ185* from now onwards) by separating the lethal mutation from the *wash*Δ185 chromosome (see Materials and Methods). *wash*Δ185* mutant females produced normal eggs and were completely fertile (Fig. 1E–I′). PCR and western blot analyses confirmed the complete loss of WASH expression in these flies (Fig. 1D). WASH was strongly expressed in wild-type ovaries, and this expression was completely lost in *wash*Δ185* mutant animals (Fig. 1D). The phenotypic analysis of homozygous *wash*Δ185* mutant developing eggs did not reveal any morphological defects (Fig. 1F,H). Phalloidin staining of developing mutant egg chambers further confirmed a wild-type morphology and organization of actin-rich structures, including ring canals and actin baskets (Fig. 1G,I). *wash* mutant egg chambers also exhibited no significant defects in border cell migration, a well-established model for invasive collective cell migration (Fig. 1J). Thus, we conclude that WASH function is not required for *Drosophila* oogenesis.

wash mutant macrophages exhibit cell spreading defects

Previous studies have highlighted an important role of WASH in efficient phagocytic and autophagic digestion in *Dictyostelium* (King et al., 2013). In *Drosophila*, different types of circulating immune cells can be found. The most abundant cell types are plasmatocytes, the professional phagocytes in flies. They fulfill similar roles as mammalian monocytes and macrophages, including phagocytosis of invading pathogens and clearance of apoptotic bodies controlling development and inflammation (Stramer et al., 2005; Wood and Jacinto, 2007). Western blot analysis confirmed specific expression of WASH in macrophage-like plasmatocytes (Fig. 2A; from here on referred to as macrophages). In these cells, WASH was most prominent at large F-actin-coated subcellular structures (Fig. 2B,B′), concentrated in the perinuclear region (Fig. 2B′). The punctate signals were absent in *wash* mutant macrophages, indicating antibody specificity (Fig. 2C).

Interestingly, we found that *wash* mutant macrophages spread properly on Concanavalin A (ConA)-coated surfaces (Fig. 2D–F), but displayed prominent defects in cell flattening and spreading on uncoated surfaces (Fig. 2C). Detailed quantification analysis confirmed a significantly reduced spreading area of both larval

Journal of Cell Science (2017) 130, 344-359 doi:10.1242/jcs.193086

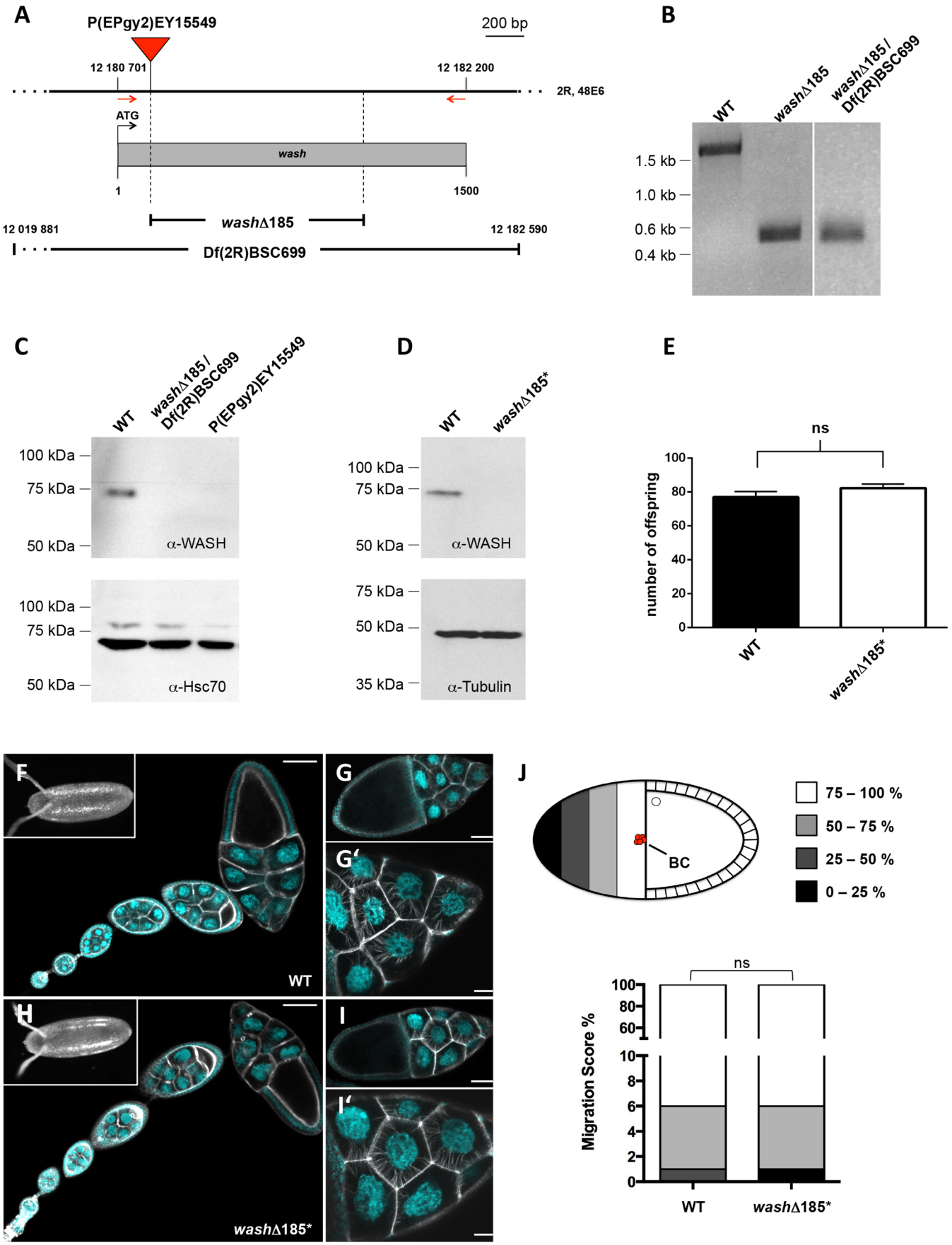

Fig. 1. See next page for legend.

Journal of Cell Science (2017) 130, 344-359 doi:10.1242/jcs.193086

Fig. 1. Homozygous *wash* mutant flies are viable and fertile. (A) Schematic overview of the *wash* gene locus. The *wash* gene comprises only one exon. The dashed lines mark the chromosomal deletion in the *wash*Δ185 mutant stock. The deficiency Df(2R)BSC699 spans the complete *wash* gene region. The insertion of the P-element used for imprecise excision is indicated by the red triangle. (B–D) PCR confirmed a deletion within *wash* of about 1 kb in *wash*Δ185 mutant flies. (B) The originally published mutant fly stock with the deficiency in trans, the stock carrying the P-element as well as the viable *wash*Δ185* stock that we established showed a complete loss of WASH expression in ovaries in western blot analysis (C,D). (E) The sterility of *wash*Δ185* female flies was tested by crossing single females with wild-type males. There was no significant difference between the number of wild-type and *wash*Δ185* offspring (*n*=111, wild type; *n*=112, *wash*Δ185*; error bars represent s.e.m.). ns, not significant. (F–I′) Egg chamber morphology was analyzed in more depth using laser scanning confocal microscopy. Neither during earlier stages of germline cyst development nor during the formation of actin baskets surrounding the nucleus in *wash*Δ185* were defects in nurse cells detected (H–I′) in comparison to the wild type (F–G′). Furthermore, the laid eggs also appeared to be wild type. Insets, bright-field micrographs of wild-type and mutant eggs are shown. (J) Quantification of border cell (BC) migration. To quantify possible defects in border cell migration in *wash*Δ185* mutants, stage-10 egg chambers were stained for F-actin (phalloidin) and nuclei (DAPI). For scoring the migration of border cell clusters, the egg chambers were divided into four regions: 75–100% migration, 50–75% migration, 25–50% migration and 0–25% migration. Scale bars: 50 µm (F–I); 20 µm (G′,I′). WT, wild type.

and pupal *wash*Δ185* macrophages on uncoated glass cover slips (Fig. 2F). Re-expression of a WASH–EGFP transgene in *wash*Δ185* mutant macrophages significantly restored cell spreading defects, indicating that the defects resulted from a loss of WASH function (Fig. 2G). Moreover, RNAi-mediated suppression of WASH and the known WASH complex components Strumpellin, SWIP, Fam21 and CCDC53 resulted in comparable spreading defects on uncoated surfaces (Fig. S1).

WASH regulates integrin-mediated cell adhesion

ConA-induced spreading is controlled by remodeling of the actin cytoskeleton upon binding of lectins to the polysaccharide side chains of plasma membrane proteins and lipids (Rogers et al., 2003); however, cell spreading on uncoated glass surfaces depends on integrin-mediated cell adhesion (Jani and Schöck, 2007). Because *wash* mutant cells spread properly on lectin-coated surfaces, we suggest that WASH plays a role in integrin-mediated cell spreading rather than in regulating lamellipodial cell protrusions. In *Drosophila*, the main β-integrin is βPS-integrin, also known as Myospheroid (Mys), which is required for cell spreading and cell migration of embryonic and pupal macrophages (Comber et al., 2013; Moreira et al., 2013). Structured illumination microscopy (SIM) revealed an overall punctate expression pattern of endogenous βPS-integrin in macrophages. The strongest signal was observed in the perinuclear region compared to a rather moderate concentration along the leading edge of the cells (Fig. 2H). *wash* mutant cells show an increased accumulation in the perinuclear region (Fig. 2I). Quantitative measurement of fluorescence intensities further confirmed an increased signal of βPS-integrin around the nuclei at the expense of peripheral staining in *wash* mutant cells (Fig. 2J).

To further stimulate integrin-mediated cell adhesion, macrophages were plated on surfaces coated with the ECM protein vitronectin. Cells spread to similar extents on vitronectin; however, they exhibited numerous βPS-integrin-positive punctae that were often enriched along the leading edge and formed prominent foci characteristic for focal adhesion sites in mammalian cells (Fig. 2K; Movie 1). Under these conditions βPS-integrin clusters colocalize with the reporter fusion protein EGFP–FAT, containing the focal targeting sequence (FAT) domain of Focal Adhesion Kinase (FAK; Fig. 2L). Stress-fiber-like actin filament bundles were seen emerging from these bright foci, as is typical for focal adhesion sites (Fig. 2L). Such dynamic focal adhesion sites were also formed *in vivo* in migrating pupal macrophages expressing EGFP–FAT imaged from prepupae (Movie 1). Similar to uncoated surfaces, *wash*Δ185* mutant cells show cell spreading defects on vitronectin (Fig. 2M). Moreover, loss of WASH function also resulted in a reduced length of vitronectin-induced cell adhesion foci along the cell periphery marked by EGFP–FAT (Fig. 2N,O; quantification in Fig. 2P; Movie 2). Thus, our data support a conserved role of *Drosophila* WASH in integrin-mediated cell adhesion.

WASH generates dynamic actin patches on endosomes

To further analyze a possible role of WASH in regulating integrin receptor trafficking, we examined the subcellular localization of WASH in *Drosophila* macrophages in more detail. WASH did not colocalize with EGFP–FAT at focal adhesion sites, suggesting that WASH itself is not a part of them but might rather regulate integrin receptor trafficking (Fig. 3A). WASH was found in close contact to βPS-integrin and surrounded βPS-integrin punctae in the perinuclear region (Fig. 3B). Live spinning disc microscopy analysis of WASH–EGFP transgene expression confirmed a dynamic localization of WASH at vesicular structures of different sizes (Fig. 3C; Movie 3). Co-expression of WASH–EGFP with Lifeact–RFP further illustrated a striking overlap of dynamic WASH and F-actin patches on these vesicles (Fig. 3D; Movie 4). Such actin patches could also be observed *in vivo* in migrating pupal macrophages that expressed Lifeact–EGFP (Movie 5). The formation of actin patches highly depends on WASH function. A wild-type macrophage showed at least two distinct actin patches on large circular vesicles, whereas loss or RNAi-mediated suppression of WASH completely abolished actin patch formation (Fig. 3E–G; quantification in Fig. 3H; Movie 6).

Further colocalization analysis with different YFP- or GFP-tagged Rab transgenes as markers for different stages of endosomal maturation revealed that actin-coated WASH vesicles mainly overlapped with small Rab4- and larger Rab7-marked endosomes, a compartment that also harbors the retromer complex (Fig. 3I–U; quantification of colocalization in Fig. 3M; Seaman and Freeman, 2014; Seaman et al., 2009). This suggests either that WASH regulates Rab4-mediated fast integrin receptor recycling from small early endosomes to the plasma membrane or that it controls recycling from a Rab7 late endosomal compartment, as previously proposed for α5β1-integrin recycling in mammalian cells (Zech et al., 2011). Consistently, we frequently found βPS-integrin punctae within Rab4- and Rab7-positive vesicles (Fig. 4A,B). Interestingly, we observed an increased accumulation of βPS-integrin in Rab7- but not in Rab4-marked endosomes in *wash* mutant macrophages (arrowheads in Fig. 4C,E). Quantification of βPS-integrin fluorescence intensity confirmed a moderate but significant increase of βPS-integrin in the lumen of late endosomes marked by endogenous Rab7 in *wash* mutant macrophages (Fig. 4F). Thus, we propose that WASH might act predominantly at that stage of late endosomal recycling of βPS-integrin in *Drosophila*, as previously suggested for α5β1-integrin recycling in mammalian cells (Zech et al., 2011).

WASH is required for cell migration of prepupal macrophages

We next analyzed a possible role of WASH in integrin-mediated cell migration *in vivo*. Previous data have revealed an important function of βPS-integrin-mediated cell adhesion in two-dimensional random cell migration in white prepupae, *in vivo* (Moreira et al., 2013). Sub-

Journal of Cell Science (2017) 130, 344-359 doi:10.1242/jcs.193086

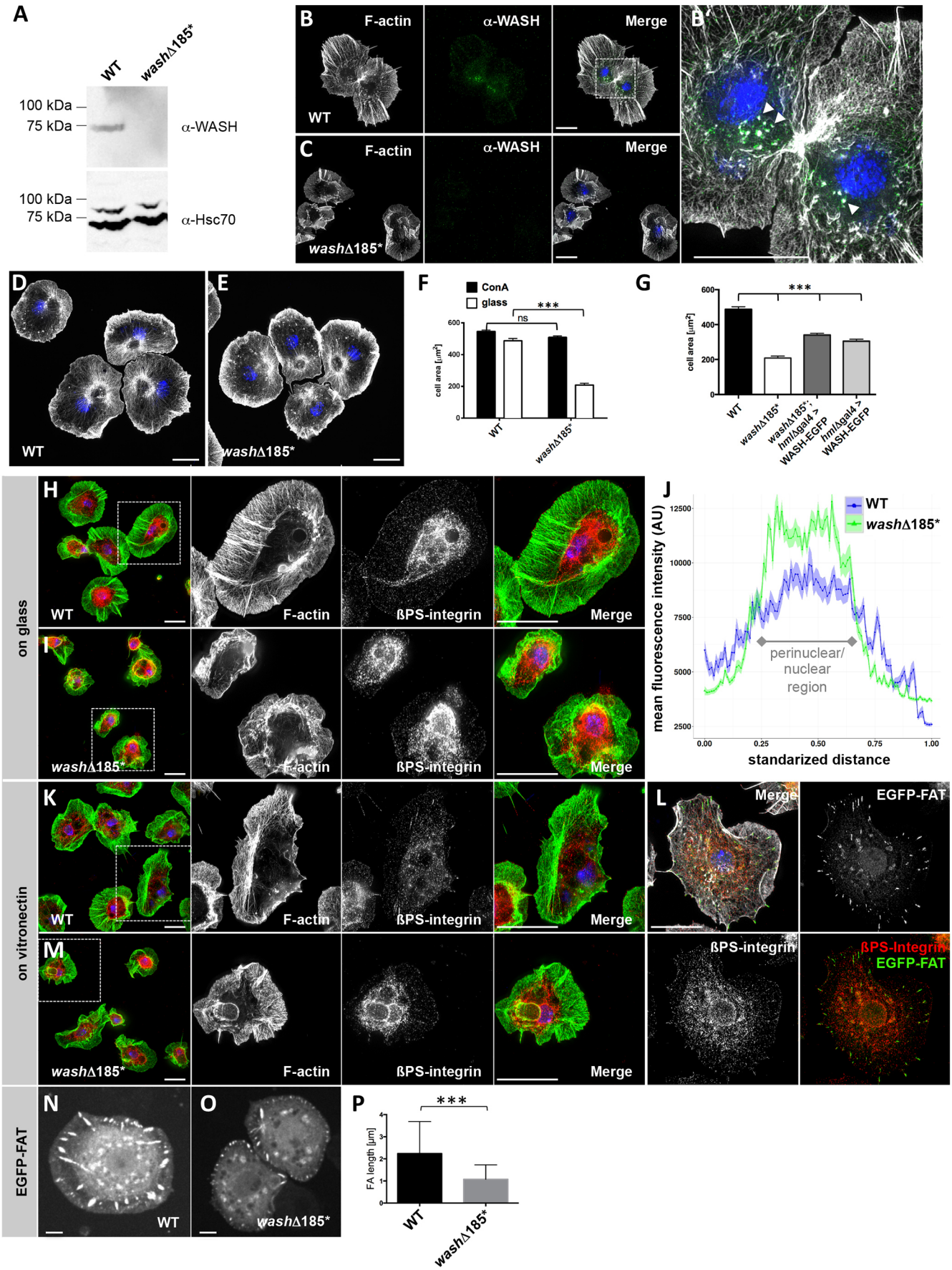

Fig. 2. See next page for legend.

Journal of Cell Science (2017) 130, 344-359 doi:10.1242/jcs.193086

Fig. 2. Loss of WASH function results in integrin-dependent cell spreading defects. (A) Western blot analysis of lysates from isolated wild-type and *wash*Δ185* macrophages confirmed a complete loss of WASH expression in mutant cells. (B–C) Structured illumination microscopy (SIM) images of isolated (B) wild-type and (C) *wash*Δ185* macrophages. Scale bars: 10 µm. (B′) In wild-type macrophages, WASH localizes to F-actin-coated subcellular structures in the perinuclear region (marked by white arrowheads). (D,E) SIM images of (D) wild-type and (E) *wash*Δ185* macrophages plated on ConA and stained for F-actin (phalloidin) and nuclei (DAPI). Scale bars: 10 µm. (F,G) Quantification of cell spreading. (F) When spread on the lectin Concavalin-A (ConA), macrophages from both wild-type and *wash*Δ185* flies spread properly. When settled on glass, *wash*Δ185* mutant macrophages exhibited spreading defects, reducing the cell area to about the half of the wild-type cell area (n=150 per genotype and treatment). The Mann–Whitney test was used for statistical analysis; ***P<0.0001 (two-tailed), error bars represent s.e.m. (G) Macrophages that re-expressed a WASH–EGFP transgene significantly restored their ability to spread. Overexpression of WASH–EGFP led to a reduction in the overall spread cell area when compared to that of wild type (n=150 per genotype). The Mann–Whitney test was used for statistical analysis; ***P<0.0001 (two-tailed), error bars represent s.e.m. (H,I) SIM images of (H) wild-type and (I) *wash*Δ185* mutant macrophages that had been stained for endogenous βPS-integrin (red), F-actin (green, phalloidin) and nuclei (blue, DAPI). Scale bars: 10 µm. (J) Quantitative measurement of fluorescence intensities revealed an increased signal of βPS-integrin around the nuclei at the expense of peripheral staining in *wash*Δ185* mutant cells. A total number of 23 wild-type and 23 washΔ185* mutant macrophages was quantified. βPS-integrin distribution was altered in *wash*Δ185* macrophages compared to in wild type. Shading represents the s.e.m. (K,M) SIM images of (K) wild-type and (M) *wash*Δ185* mutant macrophages plated on vitronectin-coated surfaces stained for endogenous βPS-integrin (red), F-actin (green, phalloidin) and nuclei (blue, DAPI). *wash*Δ185* mutant macrophages exhibit spreading defects. Note: βPS-integrin localized in distinct foci enriched along the leading edge of wild-type cells. Scale bars: 10 µm. (L) βPS-integrin-marked foci colocalized with EGFP–FAT. (N,O) Frames from spinning disc movies of (N) wild-type and (O) *wash*Δ185* mutant macrophages that expressed the focal adhesion (FA) marker EGFP–FAT. Scale bars: 10 µm. (P) Quantification of focal adhesion lengths in *wash*Δ185* macrophages compared to in wild type (***P<0.0001, error bars represent mean±s.d.). WT, wild type.

epidermal macrophages acquire a spread morphology with broad lamellipodial protrusions and collectively initiate random single cell migration (Fig. 5A, quantification in Fig. 5D–F; Movie 7; Moreira et al., 2013; Brinkmann et al., 2016). Prepupal *wash* mutant cells also showed a reduced cell spread area *in vivo* (Fig. 5D). Macrophage-specific RNAi-mediated suppression of βPS-integrin function affected cell spreading to a similar extent and nearly completely abolished cell migration (Fig. 5B, quantification in Fig. 5D–F; Movie 7). Loss of WASH function also resulted in significant albeit weaker cell migration defects with reduced migratory velocity and distance (Fig. 5C, quantification in Fig. 5E,F; Movie 7).

Additionally, we analyzed directed cell migration of macrophages upon laser-induced wounding in later pupal stages. At this stage, macrophages migrate in three dimensions rather than in two dimensions (Sander et al., 2013; Brinkmann et al., 2016). Wild-type macrophages immediately responded to a laser-ablated single cell and migrated towards the wound (ablated cell is marked by a yellow circle in Fig. 5G; Movie 8). βPS-integrin-depleted cells were able to respond and migrate towards wounds, however with strongly reduced directionality and velocity (Fig. 5H; Movie 8). By contrast, loss of WASH function had no effect on the wound response and directed cell migration during the initial phase (5–10 min after wounding; Fig. 5I; Movie 8). However, we found a reduced number of macrophages that reached the wound after 30 min by measuring the histogram-based macrophage migration score (HMMS) that we have previously established (Lammel et al., 2014; quantification in Fig. 5J). These data indicate that WASH function is important for macrophage cell motility *in vivo*.

Conserved functional and physical interactions between WASH and Vha55 V-ATPase subunit on lysosomes

Previous studies in *Dictyostelium* have revealed an important role of WASH in lysosome function. Given the localization of *Drosophila* WASH to large Rab7-positive late endosomes and/or pre-lysosomes, we further analyzed a possible conserved role of WASH in lysosome function. Mature lysosomes in macrophage-like *Drosophila* S2R^{+} cells marked by a GFP fusion with the Lysosome-associated membrane protein 1 (Lamp1) were characterized by numerous F-actin patches visualized by a Lifeact–mCherry fusion (Fig. 6A; Movie 9). We also found WASH on the surface of these large lysosomes marked by either Lamp1 or Vha55, the V-ATPase regulatory B-subunit in fixed and living cells (Du et al., 2006; Fig. 6B,C; Movies 10, 11). Strikingly, loss of WASH function in macrophages resulted in enlarged Vha55-marked lysosomes (Fig. 6D,E; quantification in Fig. 6F), suggesting a conserved role in lysosomal function. Supporting this notion, WASH can physically associate with the V-ATPase, as found in co-immunoprecipitations with a Myc-tagged Vha55 construct (Fig. 6G).

WASH function is required in phagolysosome neutralization

Based on the functional and physical interactions between WASH and the V-ATPase subunit, we further examined possible defects in phagolysosome neutralization in *wash* mutant macrophages. These cells efficiently phagocytize *Escherichia coli* particles conjugated with a pH-dependent fluorescent dye (pHrodo) within a few minutes. The fluorescence intensity of the pHrodo dye increases as the pH of its surrounding becomes acidic. Once a phagocytized pHrodo-conjugated *E. coli* enters a lysosome, the acidic environment within the phagolysosome causes a dramatic increase in fluorescent emission (Fig. 7A′; Movie 12). These phagolysosomes showed prominent actin patches (arrowheads in Fig. 7A′; Movie 12). Strikingly, WASH–EGFP was found at phagocytized *E. coli* pHrodo particles upon acidification and accumulated together with F-actin in distinct patches on phagolysosomes (Fig. 7B,C; quantification in D; Movie 13). Loss of WASH function did not affect phagocytic uptake but rather resulted in a significant defect in lysosomal neutralization (Fig. 7E,F). The neutralization defect in *wash* mutant macrophages became most obvious 60 min after phagocytic uptake (Fig. 7E,F). From this time onwards, the fluorescent emission still increased continuously in *wash* mutants, whereas in wild-type cells, the fluorescence intensity ceased after one hour (Fig. 7E,F). Thus, these data strongly support a conserved role of WASH in the retrieval of the V-ATPase from lysosomes.

Loss of WASH function promotes acidification of autophagic vesicles under starvation

Similar to the phagocytic pathway, autophagy utilizes lysosomes to degrade cytoplasm, ubiquitylated proteins or non-functional organelles. Autophagy can occur as a direct transport of selected proteins across the lysosomal membrane (microautophagy) or as an engulfment of cytoplasm and organelles by double-membrane vesicles that later on fuse with lysosomes (macroautophagy; Xie and Klionsky, 2007). Under starvation, autophagy is upregulated by the cells in order to supply the organism with nutrients (Russell et al., 2014; Xie and Klionsky, 2007).

The cellular function of WASH in lysosomal neutralization might not be restricted to the digestion of phagocytic cells such as macrophages but could also be important for starvation-induced autophagy in the *Drosophila* fat body, a nutrient storage organ analogous to the vertebrate liver. This tissue has a strong, well-characterized autophagic response to starvation, which flies use to

Journal of Cell Science (2017) 130, 344-359 doi:10.1242/jcs.193086

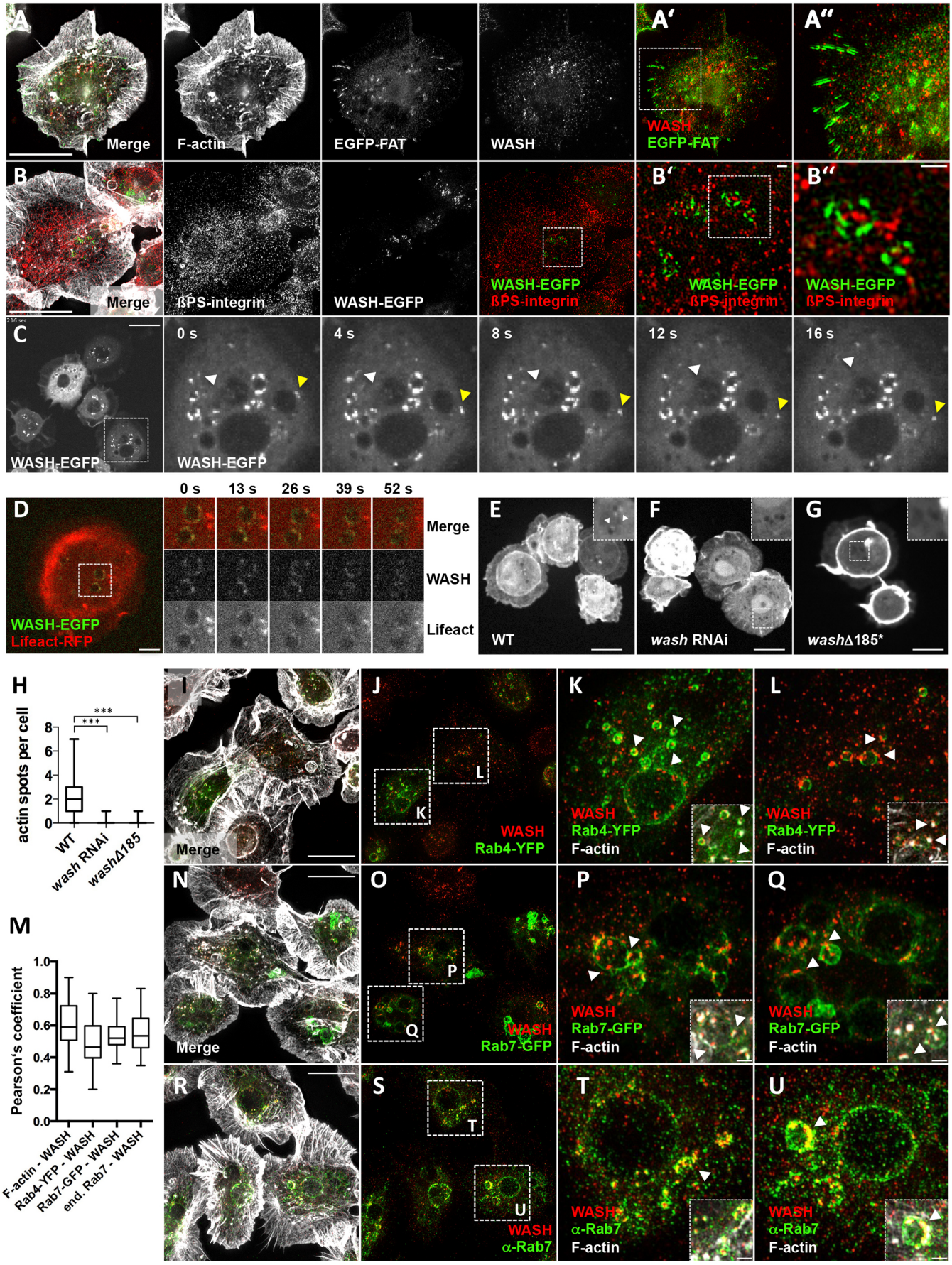

Fig. 3. See next page for legend.

Fig. 3. WASH induces dynamic actin patches on early and late endosomal vesicles. (A,A′) SIM images of a macrophage expressing the focal adhesion marker EGFP–FAT (green) and stained for endogenous WASH (red) and F-actin (white, phalloidin). WASH did not colocalize with EGFP–FAT at focal adhesion sites. White box highlights the area of the magnified inset shown in A″. Scale bar: 10 µm. (B,B″) SIM images of a wild-type macrophage expressing WASH–EGFP (green) and stained for βPS-integrin (red) and F-actin (white, phalloidin). WASH did not colocalize with EGFP–FAT at focal adhesion sites. White boxes highlight the areas of the magnified inset shown in B′ and B″. Scale bars: 10 µm (B), 1 µm (B′,B″). WASH was found in close contact to βPS-integrin and surrounded βPS-integrin punctae in the perinuclear region. (C) Still images from a spinning disc movie of wild-type macrophages expressing WASH–EGFP at indicated time points. WASH–EGFP localizes at dynamic vesicles of different sizes (small and large vesicles are marked by white and yellow arrowheads, respectively). Scale bar: 10 µm. (D) Still images from a spinning disc movie of a wild-type macrophage co-expressing WASH–EGFP with Lifeact–RFP. WASH–EGFP colocalized with F-actin at dynamic vesicles. Scale bars: 10 µm. (E–G) Still images from spinning disc movies of (E) wild-type, (F) *wash* knockdown and (G) *wash*Δ185* mutant macrophages expressing a Lifeact–EGFP transgene. Loss of WASH function results in a complete loss of actin patches (arrowheads in E). White boxes highlight the areas of the magnified insets. Scale bars: 10 µm. (H) Quantification of actin patches in macrophages of the indicated genotypes (wild type, *n*=80; *hml*Δ-Gal4>*wash*-RNAi=88; *wash*Δ185*=95). ***P<0.0001 (Mann–Whitney test). the boxes represent the 25th and 75th percentiles, whiskers represent the minimum and maximum values and the line shows the median. (I–U) SIM images of macrophages of the indicated genotypes stained for F-actin (phalloidin, white). Actin-coated WASH vesicles colocalized with small Rab4–YFP vesicles (J–L) and larger Rab7 late endosomes marked by either (O–Q) a Rab7–GFP transgene or (S–U) an anti-Rab7 antibody. White boxes highlight the areas shown in the indicated magnified insets. The arrowheads mark regions where WASH colocalized with F-actin on vesicular membranes. Scale bars: 10 µm. (M) Analysis of colocalization between WASH and F-actin (*n*=50), Rab4–YFP (*n*=58), Rab7–GFP (*n*=54) and endogenous Rab7 (*n*=40) based on Pearson's colocalization coefficient. Box and whisker plot components are as described for H.

mobilize nutrients and promote their survival. We used Lysotracker Red staining for the detection of lysosomes and autophagosomes. Fat bodies from well-fed wild-type third-instar larvae remained essentially negative for Lysotracker (Fig. 8A–C). In contrast, Lysotracker staining in the fat body of fed *wash* mutant animals was already increased (Fig. 8D–F). However, in response to amino acid starvation (sugar-only diet), we observed a more dramatic induction of enlarged punctate Lysotracker staining in mutant cells compared to in wild type (compare Fig. 8I,L). Induced autolysosomes in the *wash* mutant fat body seem to be functional given that they also showed an increased Magic Red staining, a marker for active cathepsin B, suggesting that the pH within the lysosomal lumen is more acidic promoting its hydrolytic activity during starvation-induced autophagy (Fig. 8M,N). Interestingly, WASH localizes to actin-enriched vesicular structures in the fat body cells, similar to what was observed in macrophages (Fig. 8O). These fat body structures were also marked by an Atg8–GFP transgene (Fig. 8P), a key autophagic protein that associates with autophagosomes (Shpilka et al., 2011). To further test an increased induction of functional autophagic vesicles, we analyzed Atg8 lipidation by immunoblotting of fat body lysates. Lipidation of Atg8 drives its association with the autophagosome and serves as an indicator of autophagy induction (Shpilka et al., 2011). The non-processed form (often referred to as Atg8-I) can easily be distinguished from its membrane-associated faster migrating active form (Atg8-II). Consistent with our finding that lysosomal acidity was increased in the *wash* mutant fat body, immunoblot analysis of Atg8 showed that the amount of both the non-processed and lipidated form was increased (Fig. 8Q). Thus, loss of WASH function increases starvation-induced autophagy. Finally, we examined possible changes in the life span of *wash* mutant flies under amino acid starvation. Under these conditions, *wash* mutants displayed an accelerated lethality compared to control flies (Fig. 8R). Increased lethality of starved *wash* mutant flies could be rescued by expression of the WASH–EGFP transgene in the mutant background (Fig. 8R). Thus, increased acidification of autolysosomes might shorten life span rather than promote longevity, similar to results of a recent study with WASH conditional knockout (KO) mice (Xia et al., 2013).

Taken together, our data highlight a conserved role for WASH in the endocytic sorting and recycling of membrane proteins like integrins and the V-ATPase. A loss of WASH function therefore leads to defects in cell spreading, cell motility and lysosomal neutralization. Lysosome neutralization defects in particular might contribute to a decreased life expectancy under amino acid starvation because nutrients are stuck in lysosomes and cannot nourish the starving cells or organism.

DISCUSSION

Drosophila wash was originally identified as an essential gene required for oogenesis and larval development (Linardopoulou et al., 2007; Liu et al., 2009). Our data clearly show that both larval lethality and all morphological defects of developing eggs described so far are not due to the loss of WASH function but are rather caused by a second-hit mutation. The generation of viable *wash* mutant flies bearing the same chromosomal deletion finally confirmed that WASH is dispensable for early *Drosophila* development and oogenesis. The defects in oogenesis in trans-heterozygous *wash*Δ185/*wimp* mutant flies observed by Liu et al. are probably due to the *wimp* mutation used given that *wimp* is a change-of-function mutation of an RNA polymerase II subunit and reduces maternal function of a variety of genes, including, but not limited to, *wash* (Liu et al., 2009; Parkhurst and Ish-Horowicz, 1991). Despite the apparent lack of any obvious phenotype during oogenesis, WASH seems to be expressed in *Drosophila* ovaries. Thus, redundant or compensatory pathways might mask WASH function in developing eggs. Previous expression data in wild-type flies revealed an accumulation at the oocyte cortex in addition to an overall cytoplasmic expression in all nurse and somatic follicle cells throughout oogenesis (Rodriguez-Mesa et al., 2012). The protein-A-affinity-purified monoclonal antibody (mAb P3H3; Rodriguez-Mesa et al., 2012) used in this study specifically recognizes WASH in immunoblots (Fig. 1B–D). However, in immunostainings of developing egg chambers, we found no significant differences in the expression pattern and signal intensity between wild type and mutants.

We observed a specific and prominent expression in *Drosophila* macrophages and the fat body that was completely lost in *wash* mutants. Our data strongly support a conserved role of *Drosophila* WASH as an endosome-specific NPF in regulating integrin trafficking and lysosome function. Important regulators of endosomal trafficking and recycling are Rab GTPases (Jordens et al., 2005; Wandinger-Ness and Zerial, 2014). Internalized integrin receptors enter early endosomes and can either be sorted by a 'fast' Rab4-mediated recycling pathway or transit through a 'slow' Rab11-positive recycling pathway back to the plasma membrane (Bretscher, 1992; Rainero and Norman, 2013). Our data further support previous findings of a WASH function in regulating late endosomal integrin recycling in mammalian cell culture. WASH significantly colocalized with Rab4- and Rab7-marked endosomes in macrophages. However, we only found a significant difference in βPS-integrin signals in Rab7-marked endosomes in *wash* mutant macrophages. Thus, fast Rab4-

Journal of Cell Science (2017) 130, 344-359 doi:10.1242/jcs.193086

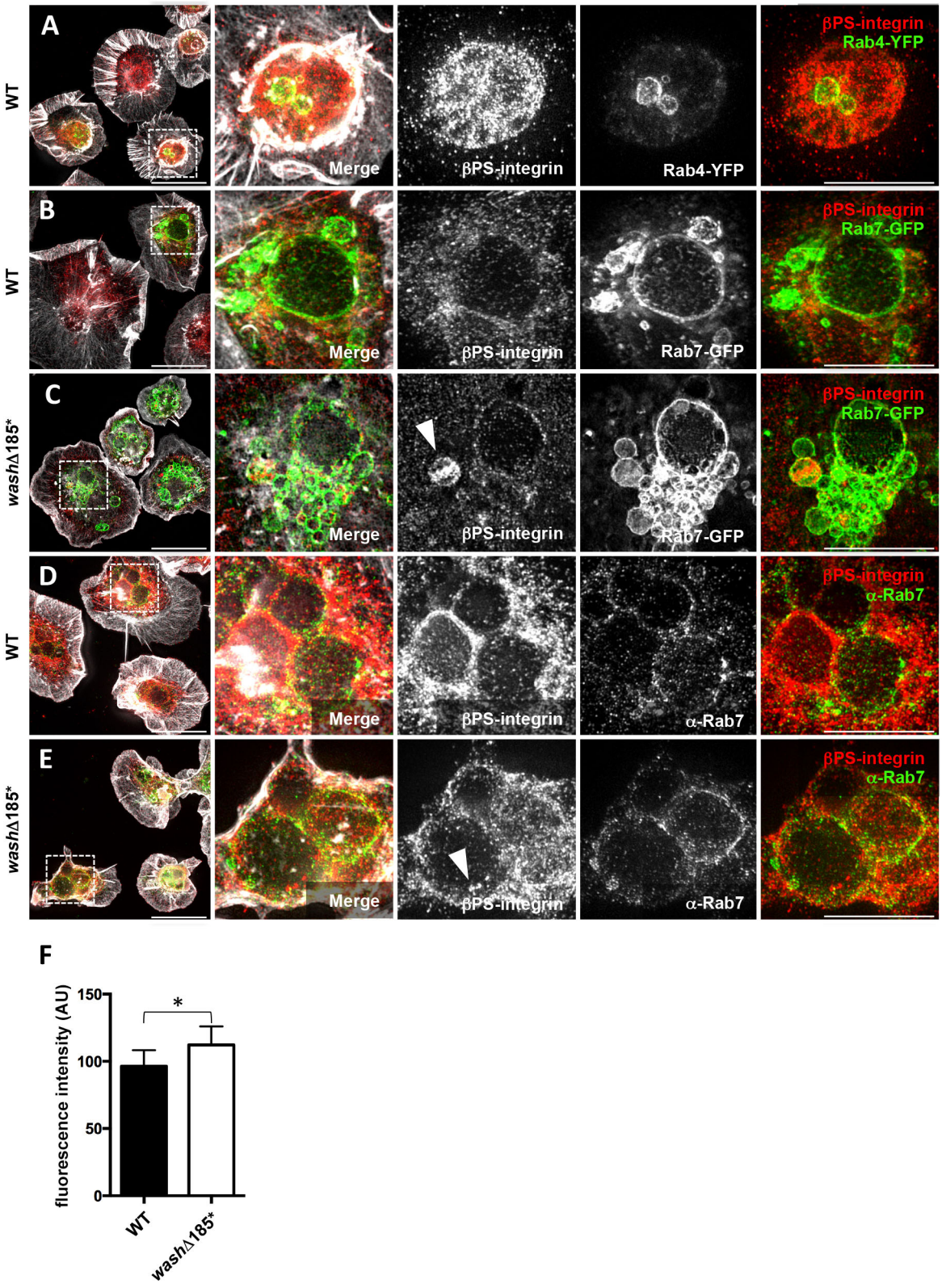

Fig. 4. Loss of WASH function results in an increased accumulation of βPS-integrin in Rab7-marked late endosomes. (A–E) SIM images of macrophages of the indicated genotypes stained for F-actin (phalloidin, white). Scale bars: 10 µm. Macrophages expressing (A) a Rab4–YFP transgene or (B) wild-type macrophages co-stained for βPS-integrin (red) and F-actin (white). βPS-integrin punctae were frequently found in the lumen of Rab4- and larger Rab7-marked vesicles. (C) Increased βPS-integrin signals are found within Rab7–GFP-positive late endosomes (arrowhead). (D,E) Endogenous Rab7 marks late endosomes in (D) wild-type and (E) *wash*Δ185* mutant macrophages with increased luminal βPS-integrin punctae (arrowheads). (F) Quantification of βPS-integrin fluorescence intensity confirmed a moderate but significant increase of βPS-integrin in the lumen of late endosomes marked by endogenous Rab7 in *wash*Δ185* mutant macrophages. A total number of six wild-type and six *wash*Δ185* mutant macrophages were imaged using SIM. 12 vesicles in wild type and 19 in *wash*Δ185* cells were analyzed using FIJI. *P<0.047 (*t*-test). Error bars represent s.e.m. WT, wild type.

Journal of Cell Science (2017) 130, 344-359 doi:10.1242/jcs.193086

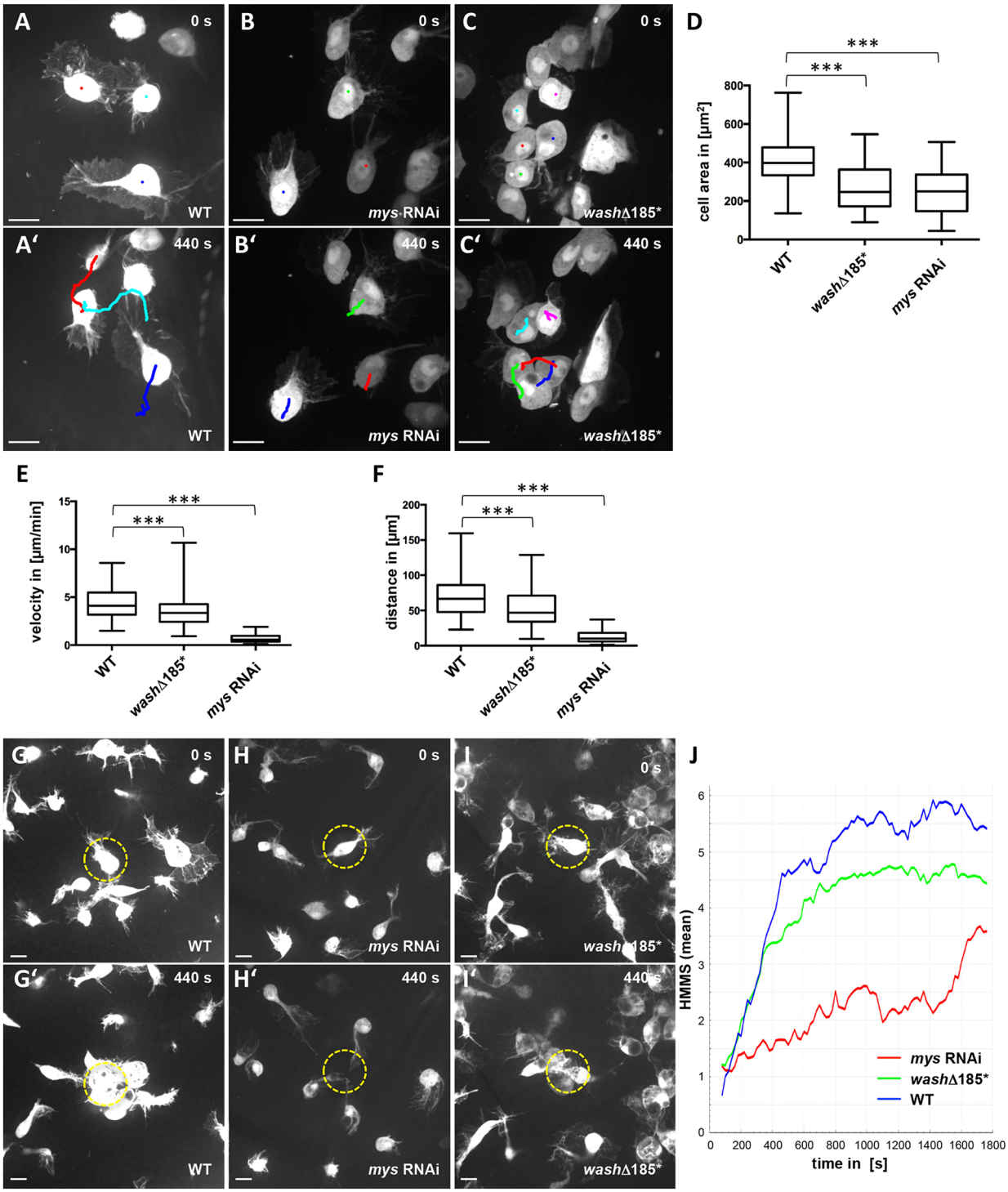

Fig. 5. WASH function is required for cell migration *in vivo*. (A–C′) Frames of spinning disc microscopy movies of migrating (A) wild-type, (B) βPS-integrin knockdown and (C) *wash*Δ185* mutant macrophages expressing an EGFP transgene imaged from a living prepupae [2 h after puparium formation (APF)]. Migratory tracks of individual cells are indicated (colored, jagged lines). Scale bars: 10 µm. RNAi-mediated suppression of βPS-integrin function strongly affected random cell migration. *wash*Δ185* mutant macrophages show reduced migration velocity and distance. (D) Quantification of cell spread area in living wild-type (*n*=55), *wash*Δ185* mutant (*n*=60) and βPS-integrin knockdown (*n*=48) prepupae (2 h APF). The *t*-test was used for statistics; ****P*<0.0001. (E,F) Quantification of the mean cell speed and distance of macrophages of the indicated genotypes; wild type, *n*=68; *wash*Δ185*, *n*=143; *mys* knockdown, *n*=64. *P*-values were calculated using Mann–Whitney test; ****P*<0.0001. (G–I′) Scale bars: 10 µm. (G,G′) Frames of a spinning disc microscopy movie of wild-type macrophages that migrate towards a laser-ablated cell (indicated by the yellow circle). (H,H′) Frames of a spinning disc microscopy movie of βPS-integrin knockdown macrophages that show a strongly impaired migratory behavior towards the wound (indicated by the yellow circle). (I,I′) *wash*Δ185* mutant macrophages responded properly towards the wound without changes in directionality and velocity. Scale bars: 10 µm. (J) Mean HMMS values for wild-type (blue, *n*=18), βPS-integrin knockdown (red=10) and *wash*Δ185* mutant (green, *n*=22) macrophages (17 h APF) determined from movies at 1800 s after wounding. An overall higher mean HMMS value was observed for the wild-type cells compared to βPS-integrin knockdown and *wash*Δ185* mutant cells. In box and whisker plots, the boxes represent the 25th and 75th percentiles, whiskers represent the minimum and maximum values and the line shows the median.

Journal of Cell Science (2017) 130, 344-359 doi:10.1242/jcs.193086

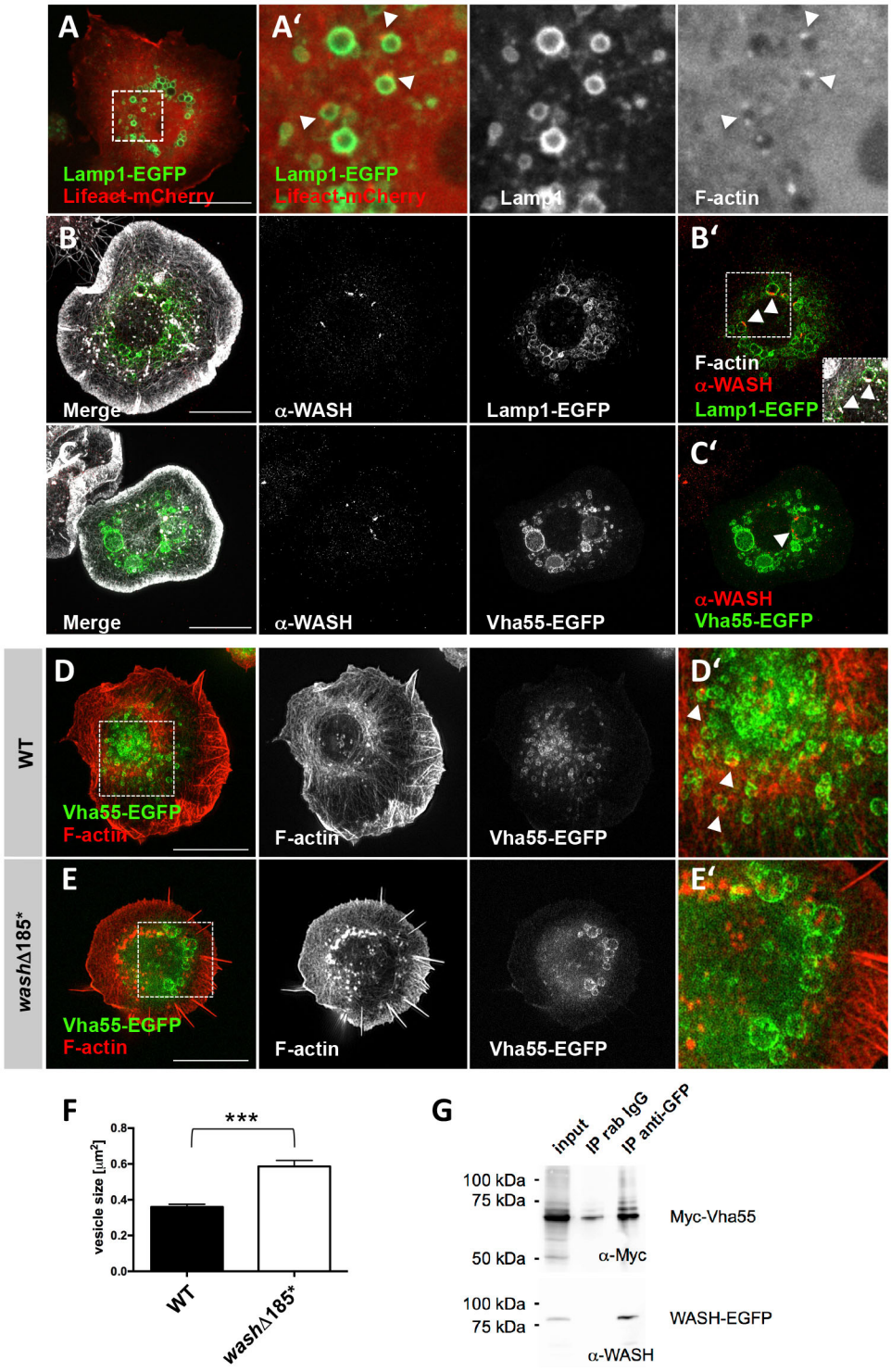

Fig. 6. WASH localizes to lysosomal vesicles in *Drosophila* macrophages as well as in S2R$^+$ cells. (A) Still images of a spinning disc movie of an S2R$^+$ cell co-expressing the lysosome-associated membrane protein Lamp1–EGFP and Lifeact–mCherry. White box highlights the area of the magnified inset shown in A. Arrowheads mark F-actin patches on Lamp1-positive lysosomes (A′). (B,C) SIM images of S2R$^+$ cells expressing (B,B′) Lamp1–EGFP (green) and (C,C′) Vha55–EGFP stained for endogenous WASH (red) and F-actin (white, phalloidin). (D,E) SIM images of isolated (D,D′) wild-type and (E,E′) *wash*Δ185* mutant macrophages expressing the V-ATPase subunit Vha55–EGFP (green) stained for F-actin (red). White boxes highlight the areas of the magnified insets. F-actin patches are present at Vha55–EGFP-positive vesicles in wild-type macrophages (arrowheads in D′). *wash*Δ185* mutant macrophages show enlarged Vha-55-marked lysosomes. Scale bars: 10 µm. (F) Quantification of Vha55–EGFP vesicle size in wild-type and *wash*Δ185* macrophages. Wild-type cells had an average size of 0.36 µm² (arrowheads, *n*=628), whereas in mutant cells, the vesicle size is increased to an average size of 0.59 µm² (*n*=549). ***P<0.0001 (Mann–Whitney test), error bars represent s.e.m. (G) Co-immunoprecipitation of WASH and Vha55 revealed that both proteins physically associate. IP, immunoprecipitation; WT, wild type.

mediated recycling of integrins might either be independent of WASH or might be masked by redundant functions of other WASP-protein family members. In summary, reduced focal adhesions, cell spreading and cell migration defects in *wash* mutant macrophages are most likely to be caused by an impaired recycling of βPS-integrin.

In wild type, receptors that are not recycled remain within early endosomes as they undergo early-to-late endosomal maturation, a step that requires the exchange of Rab5 for Rab7. Rab7 is known to recruit the retromer on endosomal membrane, and it is required for the transfer of cargo from the late endosomes to the lysosome (Priya et al., 2015; Pryor and Luzio, 2009). A conserved function of WASH in retromer-dependent endocytic recycling of the luminal protein Serpentine has already been found during *Drosophila* trachea development (Dong et al., 2013). In macrophages, WASH also associates with large circular Rab7-positive late endosomes and mature lysosomes. We found prominent actin patches that depend on WASH function on both endosomal compartments. Such localized actin patches are thought to define discrete endosomal membrane domains that facilitate protein sorting and vesicle fission

Journal of Cell Science (2017) 130, 344-359 doi:10.1242/jcs.193086

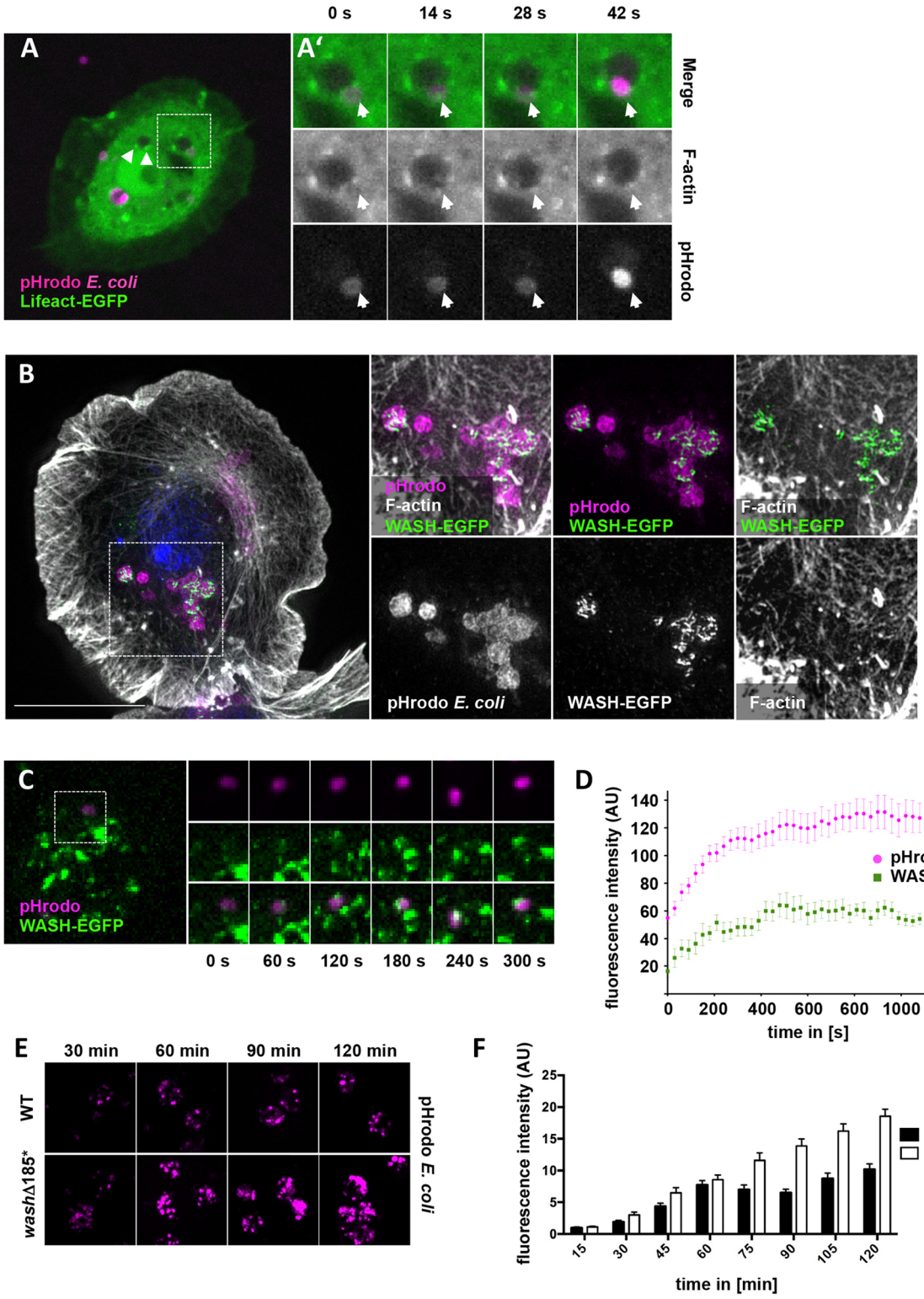

Fig. 7. WASH is required during phagocytic neutralization of macrophages. (A) Still image of a spinning disc movie of a macrophage expressing Lifeact–EGFP (green) and a phagocytosed *E. coli* particle conjugated with pH-sensitive fluorescent dye (pHrodo, magenta). Arrowheads mark F-actin patches on phagolysosomes. The white box highlights the area of the magnified insets shown in A′ at the different indicated time points. Arrows mark the phagocytosed *E. coli* particle that enters a lysosome with an increase in fluorescence intensity. (B) SIM image of a macrophage expressing WASH–EGFP (green) and phagocytosing pHrodo (magenta) shows an increase of WASH–EGFP patches at vesicles that are positive for pHrodo (magenta) and F-actin (white). Scale bar: 10 µm. (C) Still images of spinning disc movie of a macrophage expressing WASH–EGFP that is recruited to a phagocytized *E. coli* pHrodo particle upon acidification. (D) Quantification of increased WASH–EGFP and *E. coli* pHrodo fluorescence intensities over time. Error bars represent s.e.m. (E) Time course of the fluorescence intensity of phagocytized pHrodo-labeled *E. coli* particles demonstrates lysosomal neutralization defects in *wash*Δ185* macrophages. Images are taken at the indicated time points. WT, wild type. (F) Quantification of *E. coli* pHrodo particle fluorescence intensities in wild-type and *wash*Δ185* mutant macrophages over time. The mean of three independent experiments is depicted (n=7–30 cells per genotype and time point, error bars represent s.e.m.).

Journal of Cell Science (2017) 130, 344-359 doi:10.1242/jcs.193086

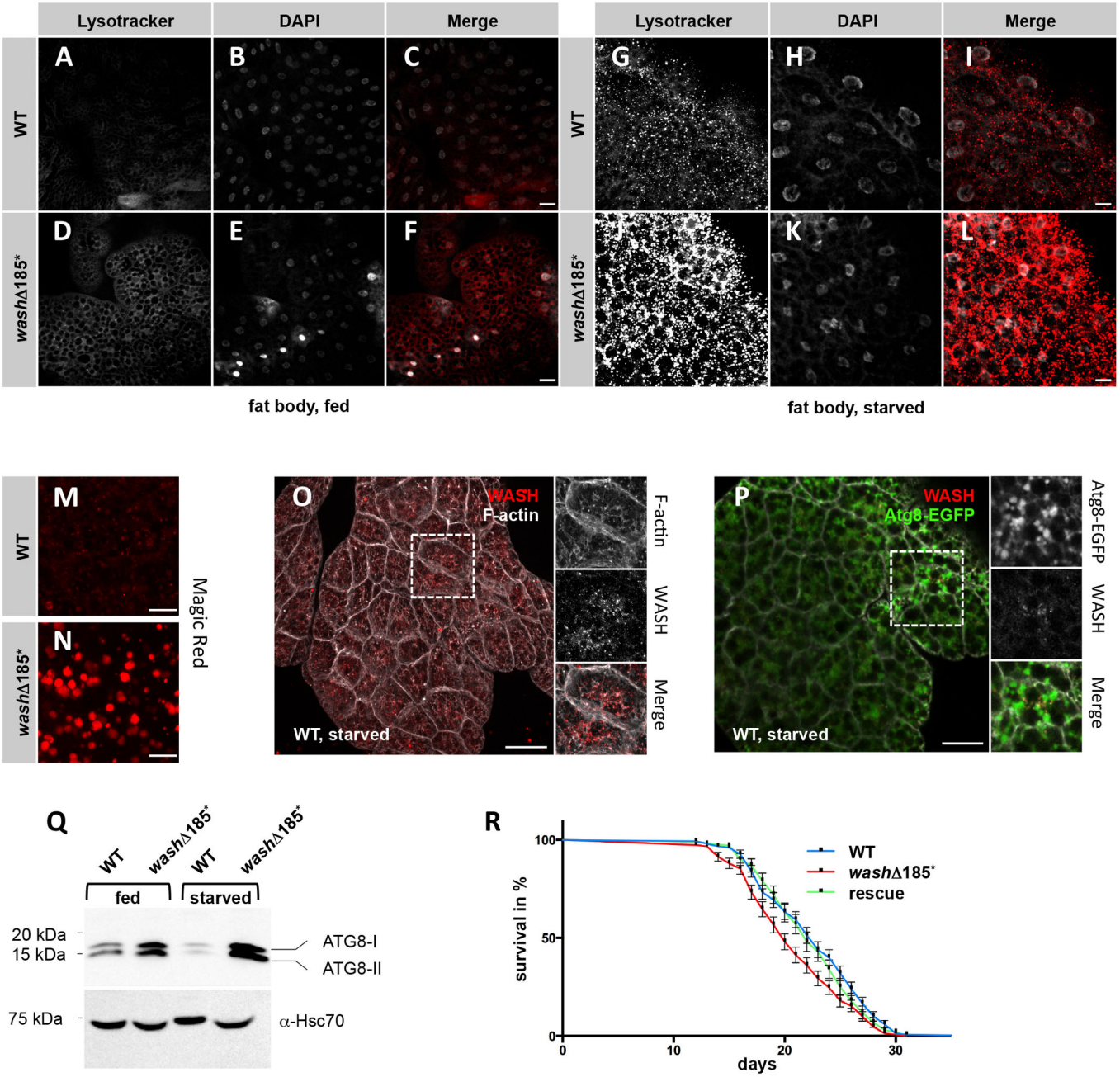

Fig. 8. Increased acidification of autophagic vesicles in *wash* mutant flies. (A–L) Confocal microscopy images of *Drosophila* fat bodies stained with Lysotracker Red of (A–C,G–I) wild-type (WT) and (D–F,J–L) *wash*Δ185* mutant larvae under fed (A–F, scale bar: 50 µm) and starved (G–L, scale bar: 20 µm) conditions. In the *wash*Δ185* mutant fat body, an increase of acidified vesicles under starved conditions could be observed. (M,N) Lysosomes in *wash* mutants seem to be functional as they are able to process cathepsin B (visualized by Magic Red staining). Scale bars: 10 µm. (O) WASH localizes to F-actin-enriched vesicular structures in the fat body cells. (P) WASH localizes at distinct domains of Atg8–EGFP-positive vesicles. Scale bars: 20 µm (O,P). (Q) The lipidation of Atg8 is also increased in the *wash*Δ185* mutant larval fat body. (R) *wash*Δ185* mutant female flies had a decreased life span compared to wild type, which can be rescued by re-expressing WASH–EGFP (the mean of three independent experiments is depicted; *n*=150, wild type and *wash*Δ185*; *n*=100, rescue; error bars represent s.e.m.).

(Derivery and Gautreau, 2010; Derivery et al., 2012, 2009; Seaman et al., 2013). Carnell and colleagues described the first mechanistic model of how WASH-dependent actin polymerization directly controls protein sorting in *Dictyostelium* lysosomes (Carnell et al., 2011). In *Dictyostelium*, WASH physically associates with the V-ATPase, a key H^+ pump that is crucial for the establishment and maintenance of the acidic pH in endosomes and lysosomes (Maxson and Grinstein, 2014). WASH directly drives the removal of V-ATPase from lysosomes and its recycling to small vesicles. Once the V-ATPase has been recycled, the lysosome becomes neutralized. Without WASH-driven actin polymerization, lysosomes never recycle V-ATPase into small vesicles and therefore do not neutralize to form post-lysosomes. Consequently, loss of WASH results in an insufficient retrieval of the V-ATPase and subsequently in an accumulation of undigested phagocytosed material that cannot be excreted by *Dictyostelium* (Carnell et al.,

Journal of Cell Science (2017) 130, 344-359 doi:10.1242/jcs.193086

2011). In this study, we have provided the first evidence that this function of WASH is not unique for *Dictyostelium* and that WASH is likely to have a conserved role in lysosome neutralization and V-ATPase recycling in higher eukaryotes such as *Drosophila*. *Drosophila* WASH binds to Vha55, the V-ATPase regulatory B-subunit, and loss of WASH function strongly affects phagolysosomal neutralization in macrophages.

Increased lysosome acidification is expected to have global effects not only on phagocytic digestion but also on autophagy, an evolutionarily conserved process that mediates the degradation of intracellular materials in lysosomes. Supporting this notion, we observed an increased starvation-induced acidification of autolysosomes that significantly reduced the life span of mutant flies. A similar, but more severe phenotype has recently been reported in *wash* knockout mice (Xia et al., 2014). WASH deficiency results in extensive autophagy that most likely causes embryonic lethality (Xia et al., 2014). Thus, WASH function inhibits rather than stimulates autophagy, as previously proposed based on RNAi cell culture experiments (Zavodszky et al., 2014a). The mechanisms promoting autophagy in mice and flies, however, seem to be different. Increased autolysosomal acidification seems to promote autophagy in *wash* mutant flies, whereas in mice, WASH might directly inhibit the formation of autophagosomes before they fuse with lysosomes to form functional autolysosomes. This direct effect of WASH on autophagosome formation is independent of its function as an NPF but seems to be mediated by inhibiting ubiquitylation of Beclin1/Atg6 (Xia et al., 2014). This tumor suppressor is part of a lipid kinase complex that mediates the initial stages of autophagosome biogenesis by recruiting other Atg proteins (Levine et al., 2015; Wirawan et al., 2012). However, Beclin1/Atg6 proteins are known to exert numerous non-autophagic functions, including protein sorting, and endocytic and phagosomal maturation (Levine et al., 2015; Wirawan et al., 2012). In flies, Atg6 is also required for multiple vesicle trafficking pathways and hematopoiesis (Shravage et al., 2013). Like in mammals, *Drosophila* Atg6 also directly interacts with the lipid kinase Vps34, and co-expression of Atg6 and Vsp34 is sufficient to induce autophagy. Consistent with its role as a tumor suppressor, loss of Atg6 function causes defects in blood cell differentiation, resulting in an overproduction of macrophages (Shravage et al., 2013). Given the inhibitory function of WASH on Beclin1/Atg6, we overexpressed WASH in flies. However, neither macrophage-specific nor ubiquitous overexpression of WASH resulted in an increased number of macrophages or the formation of melanotic blood cell masses (data not shown). Thus, gain of WASH function cannot phenocopy *atg6* mutants, suggesting distinct or more complex regulatory mechanisms in flies compared to in mammals.

MATERIALS AND METHODS

Fly genetics

All crosses were performed at 25°C unless indicated otherwise. *wash*Δ185 flies were obtained from Susan Parkhurst (Division of Basic Sciences, Fred Hutchinson Cancer Research Center, Seattle, WA) (Linardopoulou et al., 2007). Lethal mutations on the *wash*Δ185 chromosome were removed by multiple outcrossings to wild type (w1118). The following strains were used: pUASt-Vha55-EGFP (Davies et al., 1996); *hml*Δ-Gal4 (Sinenko and Mathey-Prevot, 2004); pUASt-EGFP-FAT (Sander et al., 2013), and UASt-Lifeact–EGFP, UAS-Lifeact-RFP, *Df(2R)*, P{UASp-YFP.Rab4}, P{UAS-Rab7.GFP} from the Bloomington Stock Center (IDs 26500, 58362, 9767, 24616 and 42706, respectively); RNAi lines from the Vienna *Drosophila* RNAi Center (VDRC; IDs: 24642, 39769, 24643, 107954, 31840, 23832, 110316 and 318285). Transgenic pUASt-WASH-EGFP flies were generated using ΦC31-mediated transgenesis (*M{3xP3-RFP.attP}ZH-86F*; Bischof et al., 2007).

Cell culture and cell transfection

Drosophila S2R$^+$ cells were propagated in 1× Schneider's *Drosophila* medium, as described previously (Stephan et al., 2008). S2R$^+$ cells were transfected as described previously (Bogdan et al., 2004).

Structured illumination microscopy imaging

SIM images were taken with an ELYRA S.1 microscope (CellObserver SD, 63×1.4 oil-immersion objective; Zeiss) using software ZEN 2010 D (Zeiss). Immunostaining and image acquisition were performed as previously described (Brinkmann et al., 2016; Zobel and Bogdan, 2013). Primary antibodies against the following proteins were used as follows: WASH [P3H3 from Developmental Studies Hybridoma Bank (DSHB), purified by protein-A affinity chromatography, 1:100], βPS-integrin (CF.6G11 from DSHB, 1:10); Rab7 (1:3000; Tanaka and Nakamura, 2008).

Spinning disc microscopy imaging

Live imaging of macrophage cultures was performed using a CellObserver SD spinning disc microscope (Zeiss), as reported previously (Sander et al., 2013).

Co-immunoprecipitation experiments

Co-immunoprecipitation with WASH–EGFP and Vha55–Myc were performed as previously described (Fricke et al., 2009). Western blots were stained with primary antibodies against Myc (9E10 from DSHB, 1:10) and WASH (P3H3 from DSHB, 1:100).

Sterility assay

Single female (1 day old) wild-type and *wash*Δ185* mutant flies were crossed with four male (1 day old) wild-type flies and left on *Drosophila* standard food for 7 days. 14 days after the crosses, obtained offspring were counted for each cross. The Mann–Whitney test was used for statistical analysis; P-value<0.2121 (two-tailed).

Immunohistochemistry, pHrodo uptake assay and fat body staining

For immunohistochemistry, female wild-type and *wash*Δ185* mutant flies were kept on *Drosophila* standard food supplemented with fresh yeast for 1.5 days before the ovaries were dissected. Isolated ovarioles were fixed for 15 min with 4% paraformaldehyde (Sigma Aldrich) in PBS, permeabilized for 1 h in 0.1% Triton X-100 (Invitrogen) in PBS, blocked for 30 min in 3% BSA in PBS and subsequently stained with phalloidin–Alexa-Fluor-488 and DAPI for 2 h. The *E. coli* particle pHrodo uptake assay, Lysotracker and Magic Red stainings were performed according to the manufacturers' instructions (Molecular Probes, USA).

Quantification of Vha55 vesicles, actin spots and focal adhesion length

A total number of 50 wild-type and 47 *wash*Δ185* mutant macrophages were imaged, and all Vha55-positive vesicles in a 0.5-µm stack were measured using the AxioVision SE64 Rel 4.9 software. The Mann–Whitney test was used for statistics; P-value<0.0001 (two-tailed). To quantify the number of actin spots at vesicular structures per cell, a total number of 80 wild-type, 95 *wash*Δ185* and 88 *hml*Δ-Gal4>*wash*-RNAi macrophages expressing UASt-Lifeact–EGFP were imaged. The Mann–Whitney test was used for statistical analysis; both times a P-value<0.0001 was obtained (two-tailed).

βPS-integrin fluorescence intensity in Rab7-positive vesicles and βPS-integrin distribution

To quantify the βPS-integrin immunostaining signal intensity in Rab7-positive vesicles, a total number of six wild-type and six washΔ185* mutant macrophages were imaged using SIM. 12 vesicles in wild type and 19 in washΔ185* were analyzed using FIJI. The t-test was used for statistical analysis; P-value<0.047. To quantify βPS-integrin immunostaining signal intensity and distribution, a total number of 23 wild-type and 23 *wash*Δ185* mutant macrophages were imaged using SIM. A diametrical line was drawn across each cell, thereby determining the quantification section to be used. To overcome differences in length, each line was rescaled by setting

the beginning point to 0 and the endpoint to 1. In this rescaled line, the position of each pixel was also rescaled between 0 and 1. To have relevant data for statistical purposes, the rescaled line was divided into 100 equidistant slices. The immunostaining signals within each slice were pooled, and the mean intensity was calculated. The shading represents s.e.m. For focal adhesion quantification, a total number of 75 wild-type and 53 *wash*Δ185* mutant macrophages that expressed UASt-EGFP-FAT were imaged using spinning disc microscopy and then quantified (1727 in wild type and 1346 in *wash*Δ185*) using the ZEN lite 2012 software. The Mann–Whitney test was used for statistical analysis; P-value<0.0001 (two-tailed).

In vivo migration of pupae

Live imaging of macrophages in prepupae and in the pupal wing was performed as reported recently (Sander et al., 2013; Brinkmann et al., 2016). Number of flies used for two-dimensional migration: WT (n=68), *wash*Δ185* (n=143), *hml*Δ-Gal4>*mys*-RNAi (n=64). The Mann–Whitney test was used for statistical analysis; both times a P-value<0.0001 (two-tailed) was obtained. The number of flies used for three-dimensional wound ablation: WT (n=18), *wash*Δ185* (n=22), *hml*Δ-Gal4>*mys*-RNAi (n=10).

Quantification of border cell migration

100 wild-type and 100 *wash*Δ185* mutant stage-10 egg chambers were stained for F-actin (phalloidin) and nuclei (DAPI). For scoring the migration of border cell clusters, the egg chambers were divided into four regions: 75–100% migration, 50–75% migration, 25–50% migration and 0–25% migration. The Wilcoxon matched-pairs signed-rank test was used for statistical analysis; P-value >0.9999 (two-tailed).

Acknowledgements

We thank K. Brinkmann and K. Willrodt for performing initial RNAi experiments; J. A. Dow (Institute of Molecular, Cell & Systems Biology, College of Medical, Veterinary & Life Sciences, University of Glasgow, Glasgow, UK), S. Önel (Philipps-Universität Marburg, FB Biologie, Entwicklungsbiologie, Germany) and S. Parkhurst for sharing plasmids and flies. The anti-Rab7 antibody was kindly provided by Thomas Klein (Institute of Genetics, Heinrich-Heine-Universität Düsseldorf, Germany). We also thank C. Klämbt for critical reading of the manuscript, and the Bloomington Stock Center and VDRC for fly stocks.

Competing interests

The authors declare no competing or financial interests.

Author contributions

Conceptualization: S.B.; Methodology: S.B., M.B. and B.M.N.; Formal analysis and investigation: S.B., M.B., B.M.N. and L.G.R.; Writing - original draft preparation: S.B; Writing - review and editing: S.B., B.M.N. and M.B.; Funding acquisition: S.B.; Resources: S.B., M.B. and B.M.N.; Supervision: S.B.

Funding

This work was supported by a grant to S.B. from the cluster of excellence 'Cells in Motion' (CIM; Deutsche Forschungsgemeinschaft) (BO 1890/1, BO 1890/2, BO 1890/3, BO 1890/4). S.B. was supported by the SPP1464 priority program of the Deutsche Forschungsgemeinschaft.

Supplementary information

Supplementary information available online at
http://jcs.biologists.org/lookup/doi/10.1242/jcs.193086.supplemental

References

Bischof, J., Maeda, R. K., Hediger, M., Karch, F. and Basler, K. (2007). An optimized transgenesis system for Drosophila using germ-line-specific phiC31 integrases. *Proc. Natl. Acad. Sci. USA* **104**, 3312-3317.

Bogdan, S., Grewe, O., Strunk, M., Mertens, A. and Klambt, C. (2004). Sra-1 interacts with Kette and Wasp and is required for neuronal and bristle development in Drosophila. *Development* **131**, 3981-3989.

Bretscher, M. S. (1992). Circulating integrins: alpha 5 beta 1, alpha 6 beta 4 and Mac-1, but not alpha 3 beta 1, alpha 4 beta 1 or LFA-1. *EMBO J.* **11**, 405-410.

Brinkmann, K., Winterhoff, M., Onel, S. F., Schultz, J., Faix, J. and Bogdan, S. (2016). WHAMY is a novel actin polymerase promoting myoblast fusion, macrophage cell motility and sensory organ development in Drosophila. *J. Cell Sci.* **129**, 604-620.

Carnell, M., Zech, T., Calaminus, S. D., Ura, S., Hagedorn, M., Johnston, S. A., May, R. C., Soldati, T., Machesky, L. M. and Insall, R. H. (2011). Actin polymerization driven by WASH causes V-ATPase retrieval and vesicle neutralization before exocytosis. *J. Cell Biol.* **193**, 831-839.

Comber, K., Huelsmann, S., Evans, I., Sanchez-Sanchez, B. J., Chalmers, A., Reuter, R., Wood, W. and Martin-Bermudo, M. D. (2013). A dual role for the betaPS integrin myospheroid in mediating Drosophila embryonic macrophage migration. *J. Cell Sci.* **126**, 3475-3484.

Davies, S. A., Goodwin, S. F., Kelly, D. C., Wang, Z., Sozen, M. A., Kaiser, K. and Dow, J. A. T. (1996). Analysis and inactivation of vha55, the gene encoding the vacuolar ATPase B-subunit in Drosophila melanogaster reveals a larval lethal phenotype. *J. Biol. Chem.* **271**, 30677-30684.

Derivery, E. and Gautreau, A. (2010). Evolutionary conservation of the WASH complex, an actin polymerization machine involved in endosomal fission. *Commun. Integr. Biol.* **3**, 227-230.

Derivery, E., Sousa, C., Gautier, J. J., Lombard, B., Loew, D. and Gautreau, A. (2009). The Arp2/3 activator WASH controls the fission of endosomes through a large multiprotein complex. *Dev. Cell* **17**, 712-723.

Derivery, E., Helfer, E., Henriot, V. and Gautreau, A. (2012). Actin polymerization controls the organization of WASH domains at the surface of endosomes. *PLoS ONE* **7**, e39774.

Dong, B., Kakihara, K., Otani, T., Wada, H. and Hayashi, S. (2013). Rab9 and retromer regulate retrograde trafficking of luminal protein required for epithelial tube length control. *Nat. Commun.* **4**, 1358.

Duleh, S. N. and Welch, M. D. (2010). WASH and the Arp2/3 complex regulate endosome shape and trafficking. *Cytoskeleton* **67**, 193-206.

Duleh, S. N. and Welch, M. D. (2012). Regulation of integrin trafficking, cell adhesion, and cell migration by WASH and the Arp2/3 complex. *Cytoskeleton* **69**, 1047-1058.

Du, J., Kean, L., Allan, A. K., Southall, T. D., Davies, S. A., McInerny, C. J. and Dow, J. A. T. (2006). The SzA mutations of the B subunit of the Drosophila vacuolar H+ ATPase identify conserved residues essential for function in fly and yeast. *J. Cell Sci.* **119**, 2542-2551.

Evans, I. R., Ghai, P. A., Urbančič, V., Tan, K.-L. and Wood, W. (2013). SCAR/WAVE-mediated processing of engulfed apoptotic corpses is essential for effective macrophage migration in Drosophila. *Cell Death Differ.* **20**, 709-720.

Fricke, R., Gohl, C., Dharmalingam, E., Grevelhörster, A., Zahedi, B., Harden, N., Kessels, M., Qualmann, B. and Bogdan, S. (2009). Drosophila Cip4/Toca-1 integrates membrane trafficking and actin dynamics through WASP and SCAR/WAVE. *Curr. Biol.* **19**, 1429-1437.

Gomez, T. S. and Billadeau, D. D. (2009). A FAM21-containing WASH complex regulates retromer-dependent sorting. *Dev. Cell* **17**, 699-711.

Gomez, T. S., Gorman, J. A., de Narvajas, A. A.-M., Koenig, A. O. and Billadeau, D. D. (2012). Trafficking defects in WASH-knockout fibroblasts originate from collapsed endosomal and lysosomal networks. *Mol. Biol. Cell* **23**, 3215-3228.

Harbour, M. E., Breusegem, S. Y. and Seaman, M. N. (2012). Recruitment of the endosomal WASH complex is mediated by the extended 'tail' of Fam21 binding to the retromer protein Vps35. *Biochem. j.* **442**, 209-220.

Jani, K. and Schöck, F. (2007). Zasp is required for the assembly of functional integrin adhesion sites. *J. Cell Biol.* **179**, 1583-1597.

Jia, D., Gomez, T. S., Metlagel, Z., Umetani, J., Otwinowski, Z., Rosen, M. K. and Billadeau, D. D. (2010). WASH and WAVE actin regulators of the Wiskott-Aldrich syndrome protein (WASP) family are controlled by analogous structurally related complexes. *Proc. Natl. Acad. Sci. USA* **107**, 10442-10447.

Jordens, I., Marsman, M., Kuijl, C. and Neefjes, J. (2005). Rab proteins, connecting transport and vesicle fusion. *Traffic* **6**, 1070-1077.

King, J. S., Gueho, A., Hagedorn, M., Gopaldass, N., Leuba, F., Soldati, T. and Insall, R. H. (2013). WASH is required for lysosomal recycling and efficient autophagic and phagocytic digestion. *Mol. Biol. Cell* **24**, 2714-2726.

Kolonko, M., Geffken, A. C., Blumer, T., Hagens, K., Schaible, U. E. and Hagedorn, M. (2014). WASH-driven actin polymerization is required for efficient mycobacterial phagosome maturation arrest. *Cell Microbiol.* **16**, 232-246.

Levine, B., Liu, R., Dong, X. and Zhong, Q. (2015). Beclin orthologs: integrative hubs of cell signaling, membrane trafficking, and physiology. *Trends Cell Biol.* **25**, 533-544.

Lammel, U., Bechtold, M., Risse, B., Berh, D., Fleige, A., Bunse, I., Jiang, X., Klambt, C., Bogdan, S. (2014). The Drosophila FHOD1-like formin Knittrig acts through Rok to promote stress fiber formation and directed macrophage migration during the cellular immune response. *Development* **141**, 1366-1380.

Linardopoulou, E. V., Parghi, S. S., Friedman, C., Osborn, G. E., Parkhurst, S. M. and Trask, B. J. (2007). Human subtelomeric WASH genes encode a new subclass of the WASP family. *PLoS Genet.* **3**, e237.

Liu, R., Abreu-Blanco, M. T., Barry, K. C., Linardopoulou, E. V., Osborn, G. E. and Parkhurst, S. M. (2009). Wash functions downstream of Rho and links linear and branched actin nucleation factors. *Development* **136**, 2849-2860.

Luzio, J. P., Pryor, P. R. and Bright, N. A. (2007). Lysosomes: fusion and function. *Nat. Rev. Mol. Cell Biol.* **8**, 622-632.

Maxson, M. E. and Grinstein, S. (2014). The vacuolar-type H(+)-ATPase at a glance - more than a proton pump. *J. Cell Sci.* **127**, 4987-4993.

Moreira, C. G. A., Jacinto, A. and Prag, S. (2013). Drosophila integrin adhesion complexes are essential for hemocyte migration in vivo. *Biol. Open* **2**, 795-801.

Parkhurst, S. M. and Ish-Horowicz, D. (1991). wimp, a dominant maternal-effect mutation, reduces transcription of a specific subset of segmentation genes in Drosophila. *Genes Dev.* **5**, 341-357.
Piotrowski, J. T., Gomez, T. S., Schoon, R. A., Mangalam, A. K., Billadeau, D. D. (2013). WASH knockout T cells demonstrate defective receptor trafficking, proliferation, and effector function. *Molecular and cellular biology* **33**, 958-973.
Priya, A., Kalaidzidis, I. V., Kalaidzidis, Y., Lambright, D. and Datta, S. (2015). Molecular insights into Rab7-mediated endosomal recruitment of core retromer: deciphering the role of Vps26 and Vps35. *Traffic* **16**, 68-84.
Pryor, P. R. and Luzio, J. P. (2009). Delivery of endocytosed membrane proteins to the lysosome. *Biochi. Biophys. Acta* **1793**, 615-624.
Rainero, E. and Norman, J. C. (2013). Late endosomal and lysosomal trafficking during integrin-mediated cell migration and invasion: cell matrix receptors are trafficked through the late endosomal pathway in a way that dictates how cells migrate. *Bioessays* **35**, 523-532.
Rodriguez-Mesa, E., Abreu-Blanco, M. T., Rosales-Nieves, A. E. and Parkhurst, S. M. (2012). Developmental expression of Drosophila Wiskott-Aldrich Syndrome family proteins. *Dev. Dyn.* **241**, 608-626.
Rogers, S. L., Wiedemann, U., Stuurman, N. and Vale, R. D. (2003). Molecular requirements for actin-based lamella formation in Drosophila S2 cells. *J. Cell Biol.* **162**, 1079-1088.
Russell, R. C., Yuan, H.-X. and Guan, K.-L. (2014). Autophagy regulation by nutrient signaling. *Cell Res.* **24**, 42-57.
Sander, M., Squarr, A. J., Risse, B., Jiang, X. and Bogdan, S. (2013). Drosophila pupal macrophages – a versatile tool for combined ex vivo and in vivo imaging of actin dynamics at high resolution. *Eur. J. Cell Biol.* **92**, 349-354.
Seaman, M. N. J. and Freeman, C. L. (2014). Analysis of the Retromer complex-WASH complex interaction illuminates new avenues to explore in Parkinson disease. *Commun. Integr. Biol.* **7**, e29483.
Seaman, M. N. J., Harbour, M. E., Tattersall, D., Read, E. and Bright, N. (2009). Membrane recruitment of the cargo-selective retromer subcomplex is catalysed by the small GTPase Rab7 and inhibited by the Rab-GAP TBC1D5. *J. Cell Sci.* **122**, 2371-2382.
Seaman, M. N. J., Gautreau, A. and Billadeau, D. D. (2013). Retromer-mediated endosomal protein sorting: all WASHed up! *Trends Cell Biol.* **23**, 522-528.
Shpilka, T., Weidberg, H., Pietrokovski, S. and Elazar, Z. (2011). Atg8: an autophagy-related ubiquitin-like protein family. *Genome Biol.* **12**, 226.
Shravage, B. V., Hill, J. H., Powers, C. M., Wu, L. and Baehrecke, E. H. (2013). Atg6 is required for multiple vesicle trafficking pathways and hematopoiesis in Drosophila. *Development* **140**, 1321-1329.
Sinenko, S. A. and Mathey-Prevot, B. (2004). Increased expression of Drosophila tetraspanin, Tsp68C, suppresses the abnormal proliferation of ytr-deficient and Ras/Raf-activated hemocytes. *Oncogene* **23**, 9120-9128.
Stephan, R., Grevelhörster, A., Wenderdel, S., Klämbt, C. and Bogdan, S. (2008). Abi induces ectopic sensory organ formation by stimulating EGFR signaling. *Mech. Dev.* **125**, 183-195.
Stramer, B., Wood, W., Galko, M. J., Redd, M. J., Jacinto, A., Parkhurst, S. M. and Martin, P. (2005). Live imaging of wound inflammation in Drosophila embryos reveals key roles for small GTPases during in vivo cell migration. *J. Cell Biol.* **168**, 567-573.
Tanaka, T. and Nakamura, A. (2008). The endocytic pathway acts downstream of Oskar in Drosophila germ plasm assembly. *Development* **135**, 1107-1117.
Veltman, D. M. and Insall, R. H. (2010). WASP family proteins: their evolution and its physiological implications. *Mol. Biol. Cell* **21**, 2880-2893.
Verboon, J. M., Rahe, T. K., Rodriguez-Mesa, E. and Parkhurst, S. M. (2015). Wash functions downstream of Rho1 GTPase in a subset of Drosophila immune cell developmental migrations. *Mol. Biol. Cell* **26**, 1665-1674.
Wandinger-Ness, A. and Zerial, M. (2014). Rab proteins and the compartmentalization of the endosomal system. *Cold Spring Harb. Perspect. Biol.* **6**, a022616.
Wirawan, E., Lippens, S., Vanden Berghe, T., Romagnoli, A., Fimia, G. M., Piacentini, M. and Vandenabeele, P. (2012). Beclin1: a role in membrane dynamics and beyond. *Autophagy* **8**, 6-17.
Wood, W. and Jacinto, A. (2007). Drosophila melanogaster embryonic haemocytes: masters of multitasking. *Nat. Rev. Mol. Cell Biol.* **8**, 542-551.
Xia, P., Wang, S., Du, Y., Zhao, Z., Shi, L., Sun, L., Huang, G., Ye, B., Li, C., Dai, Z. et al. (2013). WASH inhibits autophagy through suppression of Beclin 1 ubiquitination. *EMBO J.* **32**, 2685-2696.
Xia, P., Wang, S., Huang, G., Du, Y., Zhu, P., Li, M. and Fan, Z. (2014). RNF2 is recruited by WASH to ubiquitinate AMBRA1 leading to downregulation of autophagy. *Cell Res.* **24**, 943-958.
Xie, Z. and Klionsky, D. J. (2007). Autophagosome formation: core machinery and adaptations. *Nat. Cell Biol.* **9**, 1102-1109.
Zavodszky, E., Seaman, M. N. J., Moreau, K., Jimenez-Sanchez, M., Breusegem, S. Y., Harbour, M. E. and Rubinsztein, D. C. (2014a). Mutation in VPS35 associated with Parkinson's disease impairs WASH complex association and inhibits autophagy. *Nat. Commun.* **5**, 3828.
Zavodszky, E., Seaman, M. N. J. and Rubinsztein, D. C. (2014b). VPS35 Parkinson mutation impairs autophagy via WASH. *Cell Cycle* **13**, 2155-2156.
Zech, T., Calaminus, S. D. J., Caswell, P., Spence, H. J., Carnell, M., Insall, R. H., Norman, J. and Machesky, L. M. (2011). The Arp2/3 activator WASH regulates alpha5beta1-integrin-mediated invasive migration. *J. Cell Sci.* **124**, 3753-3759.
Zobel, T. and Bogdan, S. (2013). A high resolution view of the fly actin cytoskeleton lacking a functional WAVE complex. *J. Microsc.* **251**, 224-231.

Supplementary material

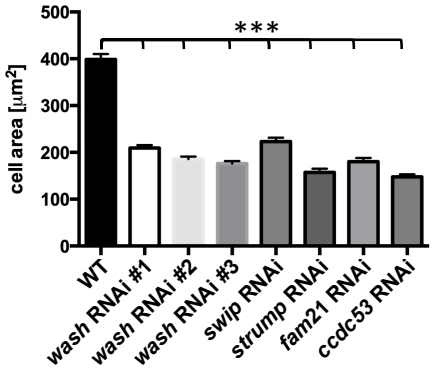

Supplementary figure S1
WASH is associated in a pentameric complex whose stability depends on each member. When single complex members are knocked down by RNAi, macrophages are unable to spread properly, comparable to the *wash* mutant situation (n = 200 per genotype). *** = $p < 0.0001$, error bars represent SEM.

Journal of Cell Science • Supplementary information

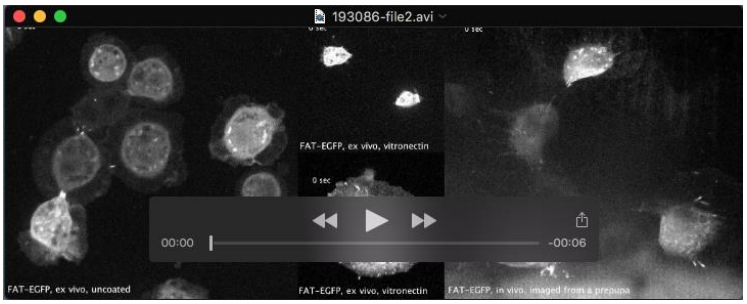

Supplementary Movie M1

Spinning disc microscopy time-lapse movie of macrophages expressing EGFP- FAT using the *hml*ΔGal4 driver *ex vivo* plated on coated and uncoated surfaces, as well as *in vivo* in a prepupa.

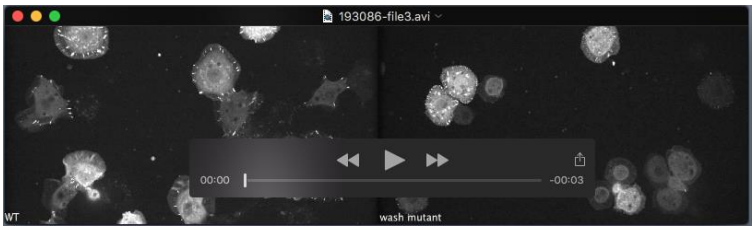

Supplementary Movie M2

Spinning disc microscopy time-lapse movie of *ex vivo* cultured wild type and *wash*Δ185* mutant macrophages expressing EGFP-FAT using the *hml*ΔGal4 driver.

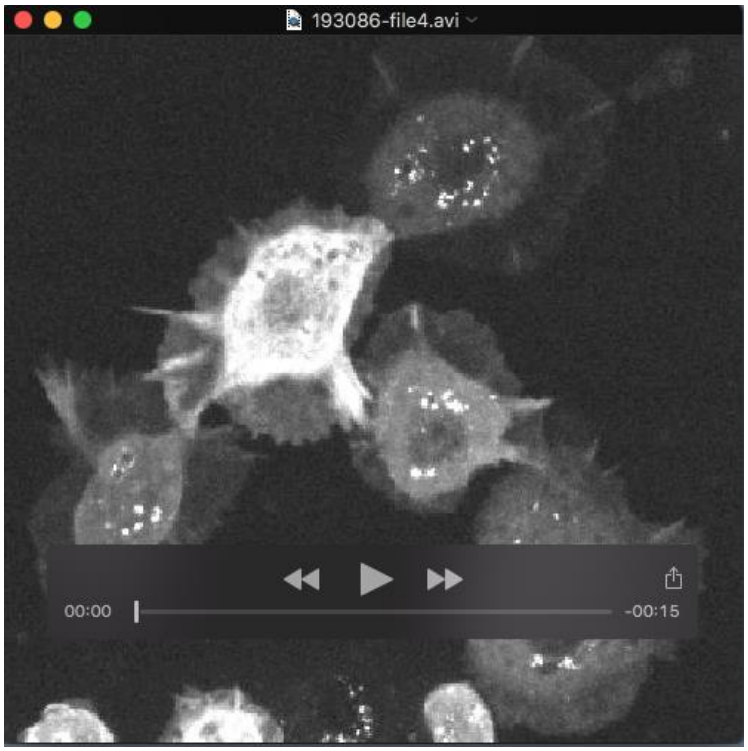

Supplementary Movie M3

Spinning disc microscopy time-lapse movie of *ex vivo* cultured macrophages expressing WASH-EGFP using the *hml*ΔGal4 driver.

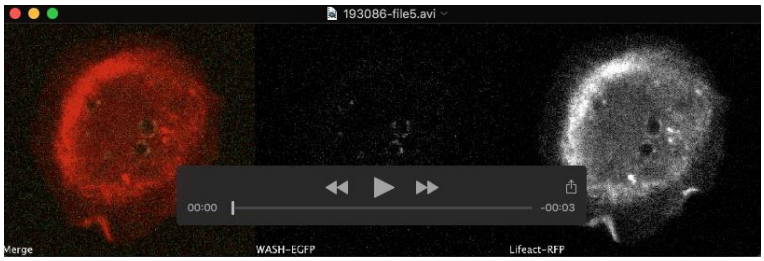

Supplementary Movie M4

Spinning disc microscopy time-lapse movie of *ex vivo* cultured macrophages expressing WASH-EGFP and Lifeact-RFP using the *hml*ΔGal4 driver.

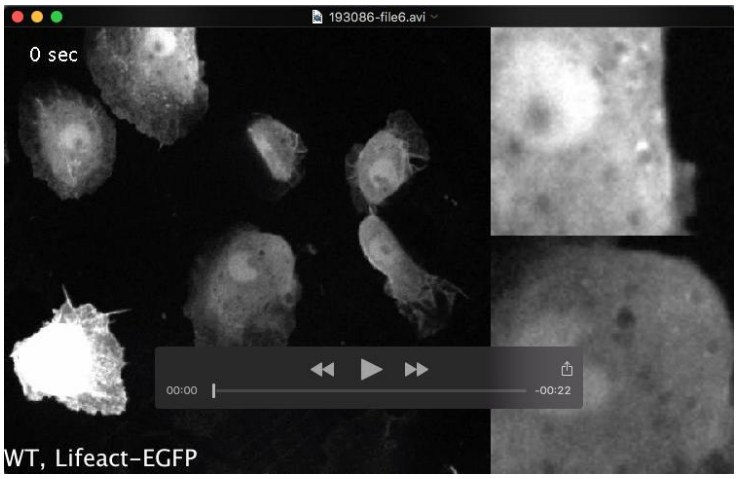

Supplementary Movie M5

Spinning disc microscopy time-lapse movie of *ex vivo* cultured macrophages expressing Lifeact-EGFP using the *hml*ΔGal4 driver.

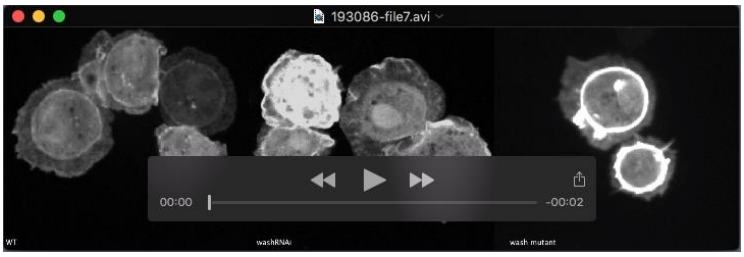

Supplementary Movie M6

Spinning disc microscopy time-lapse movie of *ex vivo* cultured (A) wild type (B) *wash*RNAi depleted and (C) *wash*Δ185* mutant macrophages expressing Lifeact-EGFP using the *hml*ΔGal4 driver.

Journal of Cell Science • Supplementary information

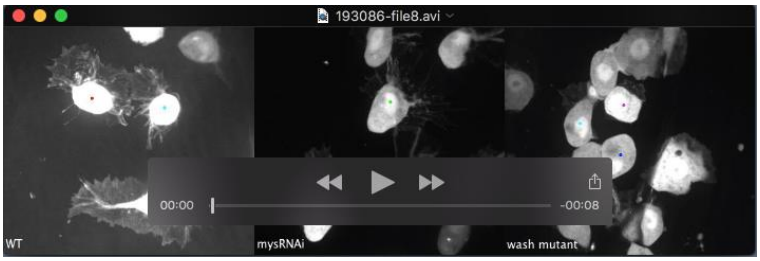

Supplementary Movie M7

Spinning disc microscopy video of migrating (A) wild type, (B) βPS-integrin knockdown and (C) *wash*Δ185* mutant macrophages expressing a EGFP transgene imaged from a living prepupa (2 h APF). Migratory tracks of individual cells are indicated (colored, jagged lines).

Journal of Cell Science • Supplementary information

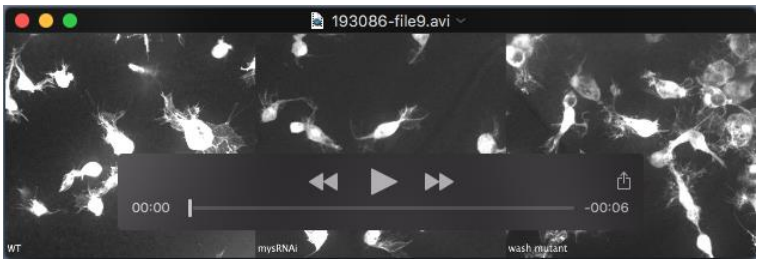

Supplementary Movie M8

Spinning disc microscopy video of migrating (A) wild type, (B) βPS-integrin knockdown and (C) *wash*Δ185* mutant macrophages expressing a EGFP transgene imaged from a pupal wing (17 h APF) upon laser-induced cell ablation.

Journal of Cell Science • Supplementary information

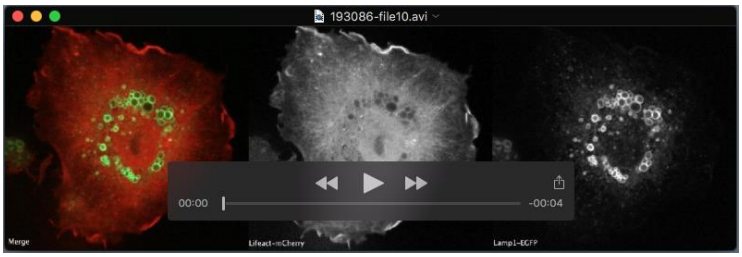

Supplementary Movie M9

Spinning disc microscopy time-lapse movie of cultured S2R^{+} cells transfected with Lifeact-mCherry and Lamp1-EGFP.

Supplementary Movie M10

Spinning disc microscopy time-lapse movie of cultured S2R^{+} cells transfected with WASH-mCherry and Lamp1-EGFP.

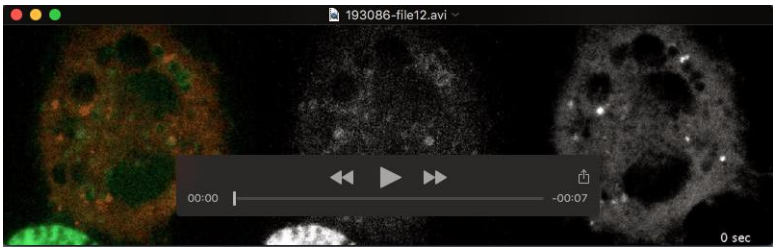

Supplementary Movie M11

Spinning disc microscopy time-lapse movie of cultured S2R^{+} cells transfected with WASH-mCherry and Vha55-EGFP.

Supplementary Movie M12

Spinning disc microscopy time-lapse movie of an *ex vivo* cultured macrophage expressing Lifeact-EGFP using the *hml*ΔGal4 driver phagocytosing pHrodo-conjugated *E. coli*

Supplementary Movie M13

Spinning disc microscopy time-lapse movie of an *ex vivo* cultured macrophage expressing WASH-EGFP (green) and phagocytosing pHrodo (magenta). WASH-EGFP is recruited to phagolysosomes with internalized *E. coli* pHrodo particles upon acidification.

Journal of Cell Science • Supplementary information